A review on the mechanical behaviour of microcellular and nanocellular polymeric foams: what is the effect of the cell size reduction?

Louise Le Barbenchon, Jean-Benoît Kopp

Journal of Cellular Plastics
XX(X):1–26

DOI: 10.1177/ToBeAssigned
www.sagepub.com/
SAGE

A review on the mechanical behaviour of microcellular and nanocellular polymeric foams: what is the effect of the cell size reduction?

Louise Le Barbenchon[1] and Jean-Benoît Kopp[1]

Abstract

Research on nanocellular foams is motivated in part by the promise of physical properties, in particular mechanical properties, that can go beyond the classical mechanical framework. However, due to the difficulty in obtaining foams of a given density but different cell sizes, determining the effect of cell size on the mechanical properties of polymer foams remains a challenge. To overcome this difficulty, studies on the mechanical behaviour of mesocellular, microcellular and nanocellular polymer foams have been compiled in this review article. After describing the different cellular structures between meso-, micro- and nanocellular foams, the mechanical properties are examined as a function of relative density and cell size. It is shown that for small strains and at low strain rates, nanocellular foams exhibit mechanical behaviour predicted by the Gibson and Ashby model. Relative density remains the first important factor to be taken into account when studying the Young's modulus and buckling stress of nanocellular foams. The focus then shifts to fracture properties, as microcellular foams have already been shown to be far superior to more conventional foams. As studies are still scarce and different methodologies have been used, no general conclusions can be drawn. However, the fracture and impact properties could be greatly improved by this change in scale. The local confinement of molecular chains in polymeric nanocellular foams or the relaxation of the triaxial stress state in front of the crack tip could explain these observations.

Keywords

Cellular material, Plastic foam, Nanocellular foam, Microcellular foam, Mechanical Behaviour, Fracture

Nomenclature

ε_d	Strain at the onset of the densification
E_s	Young's modulus of the constitutive material
E^*	Young's modulus of the foam
ϕ	Volume fraction of the solid contained in the edges of the cell
K_I	Stress intensity factor
K_{Ic}	Fracture toughness
K_{Ics}	Fracture toughness of the dense material
K^*_{Ic}	Fracture toughness of the foam
ν^*	Poisson's ratio of the foam
$\overline{n}$	Average number of edges per face
N_c	Cell density
p_0	Inner pressure of the cells
p_{at}	Atmospheric pressure
ρ	Density
ρ^*	Foam density
ρ_s	Constitutive material density
ρ_r	Relative density
σ_{fs}	Failure strength of the constitutive material
σ_{ys}	Yield strength of the constitutive material
σ^*_{pl}	Buckling stress of elasto-plastic foams
t_e	Edges thickness
t_f	Faces thickness
X	Foam expansion ratio
Z_f	Number of faces meeting on an edge

Abbreviations and acronyms

ABS	Acrylonitrile butadiene styrene
CPET	Crystallized poly(ethy1ene terephthalate)
DMA	Dynamic mechanical analysis
EPFM	Elastic plastic fracture mechanics
FPZ	Fracture process zone
LDPE	Low-density polyethylene
LEFM	Linear elastic fracture mechanics
MAM	PMMA-co-PBA-co-PMMA block copolymer
PBA	Poly(butyl acrylate)
PC	Polycarbonate
PEI	Polyetherimide
PESF	Poly(ether sulfone)
PLA	Poly(lactic acid)
PMI	Polymethacrylimide
PMMA	Poly(methyl methacrylate)
PMMA-sep	PMMA with sepiolite inclusions
PPSF	Poly(phenyl sulfone)
PS	Polystyrene
PS-PFS	Poly[styrene-block-4-(perfluorooctylpropyloxy)styrene]
PU	Polyurethane
PVC	Poly(vinyl chloride)
RPU	Rigid polyurethane
$scCO_2$	Supercritical CO_2
SEM	Scanning electron microscopy
TPU	Thermoplastic polyurethane

[1] Arts et Métiers ParisTech, Univ. Bordeaux, Bordeaux INP, CNRS, I2M, UMR 5295, 33000 Bordeaux, France

Corresponding author:
Louise Le Barbenchon, Esplanade des Arts et Métiers, Institute of Mechanics and Mechanical Enginering, 33405 Talence, France.
Email: louise.le-barbenchon@u-bordeaux.fr

Introduction

New materials are being developed since the copper age (10 000 BC) to fill the material property space (1). Very low density materials with a density between 10 and 30 kg m^{-3} could finally be obtained with the development of synthetic foams during the 20^{th} century (2) (fig. 1). Cellular polymers have since found great popularity and have been used in a wide range of applications such as the automotive industry (3) and more globally in the transport, sport (4) or packaging (5). Cellular polymers, also called foamed plastics are sought after for their light weight, low thermal conductivity and energy absorption properties for vibration damping and under impact.

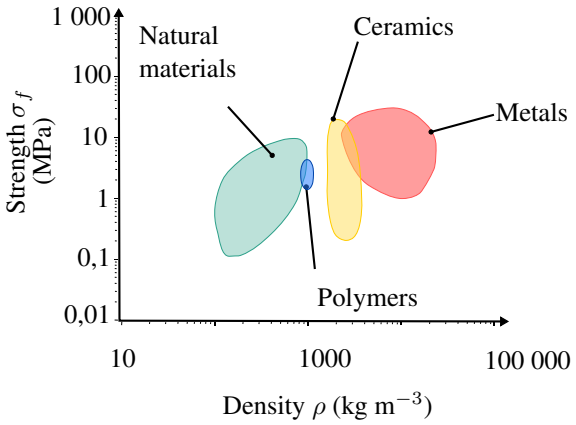

(a) Early 20^{th} century

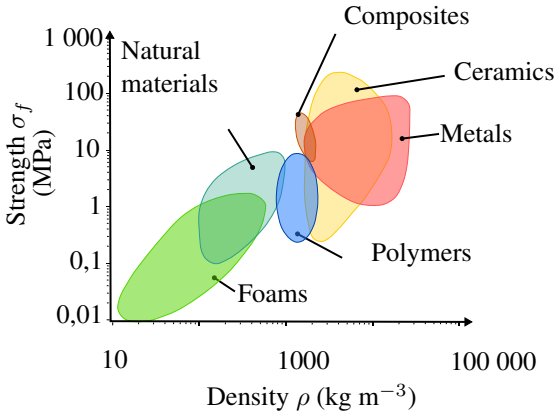

(b) Nowadays

Figure 1. Progressive filling of the material space over time, adapted from (1), courtesy of the Royal Society Publishing (log-log scale).

Because of their porous nature, foams are usually compared with their constitutive material. They are thus characterised by their relative density ρ_r, given by

$$\rho_r = \frac{\rho^*}{\rho_s}, \tag{1}$$

or their expansion ratio X, expressed as

$$X = \frac{\rho_s}{\rho^*} = \frac{1}{\rho_r}, \tag{2}$$

with ρ^*, the density of the foam and ρ_s, the density of the dense constitutive material of the foam or the density of the unfoamed material. It has been shown to be the main parameter to consider when predicting the mechanical behaviour of foams (6).

With the introduction of new manufacturing processes allowing to obtain cellular materials with controlled and micrometric porosities (1 - 100 μm), it was expected that the physical properties of the microcellular foams would be improved in an exceptional way (7). Several studies have shown that the basic mechanical properties of microcellular plastics, such as their Young's modulus or their tensile strength, are proportional to their relative density (8; 9; 10), in agreement with the micromechanical model proposed by Gibson and Ashby (6). Therefore, the reduction in cell size had not the expected effect on the mechanical properties of microcellular plastics: the relative density-related mechanical properties of microcellular plastics do not exhibit a significant superiority over their mesocellular counterparts. The relative density ρ_r remains the first order parameter influencing the mechanical behaviour of microcellular foams.

Since then, several research teams have been working on reducing the size of the pores and nanoscopic porosities were finally achieved at the beginning of the 21^{th} century (11; 12; 13; 14; 15; 16; 17; 18). Recently, Martin-de-Leon et al. achieved a characteristic cell size of around 20 nm (19). Their physical properties such as their mechanical and thermal behaviour (20; 21) have been studied and seem to indicate better properties than their microcellular counterparts. However, due to the difficulty in obtaining foams of a given density but different cell sizes, determining the effect of cell size on the mechanical properties of polymer foams remains a challenge. Therefore, to further investigate the influence of cell size on the mechanical behaviour of mesocellular to nanocellular plastics, it is necessary to take into account both the cell size and the relative density when analysing the results.

In this review article, we propose to quickly summarise the fabrication processes of nanocellular plastics and their resulting cellular structure. The review will then focus on the mechanical properties of these materials, with the associated mechanical models that have been developed over the years. A comparison of the studies on the mechanical properties in compression and at fracture will be carried out in order to study the influence of the cell size on these mechanical properties. Finally, a discussion is proposed to explain why nanocellular plastics seem to display a better fracture and impact behaviour than foams with larger porosities. Thin film effect and the triaxial stress state of cellular plastics are discussed.

Towards nanocellular foams

Since the 80's, various processes have been used to produce microcellular structures (7; 22; 23; 24; 25; 26; 27). The transition from micro to nano has been gradual. Supercritical CO_2 ($scCO_2$), a blowing agent

already used to produce microcellular foams (25; 28), was proved to be the most suitable production route for nanocellular foams (14; 29; 30). In comparison to microcellular foams, the novelty for nanocellular foams consists in the addition of block copolymers with CO_2-philic blocks within the polymer (31; 32). Depending on the polymer, this copolymer is modified. In the case of polystyrene (PS), spherical nanodomains of fluorinated CO_2-philic blocks are added. A film of poly[styrene-block-4-(perfluorooctylpropyloxy)styrene] (PS-PFS) is thus expanded to obtain a nanocellular structure (12).

In the case of poly(methyl methacrylate) (PMMA), a triblock copolymer called MAM (PMMA-co-PBA-co-PMMA block copolymer where PBA is poly(butyl acrylate)) organised in nanoscopic micelles is dispersed in varying amounts in the polymer. MAM is known to homogenise the cell size distribution and generally tends to decrease the cell size of PMMA foams in batch processes (33; 34; 15). PMMA/MAM is a good model system, that is why many research works studied the batch foaming process of this mixture varying the process parameters (31; 35; 29; 36; 37; 38). These works indicate that the accessible density is between 1 and 0.25 10^3 kg m^{-3} (representing a relative density between respectively 0.83 and 0.21). The average cell size is generally between several tens of micrometers to 0.1 μm, but can reach 50 nm thanks to saturation conditions at very low temperatures (0 to -32°C) (39; 40; 41) or very high pressures (10 to 30 MPa) (15; 32; 42; 43; 21). Indeed, a decrease in temperature or an increase in pressure increases the CO_2 mass uptake. This promotes nucleation within the material and thus the apparition of high cellular density and nanoscopic porosities. Furthermore at low temperature, no coalescence happens which allows a small cell size (43). Other methods are also used to increase the cell density and to decrease the cell size like the addition of nanocomposites (16; 44; 45; 46) or the cold crystallization phenomenon in poly(lactic acid) (PLA) (47; 48).

It can be noted that all the processes presented for the nanocellular materials are always batch processes. In batch processes, CO_2-saturation is of the order of a few hours. If one wish to industrialise these nanocellular foams like the microcellular foams, the use of semi-continuous or even continuous processes is therefore necessary (14; 38). However, in continuous processes, rheology, thermodynamics, sorption/desorption/diffusion kinetics and the final foaming are intrinsically coupled. Controlling these phenomena in a very short time stays today an underlying scientific problem, as noted in previous studies (49; 50).

Description of the cellular structures

As for natural materials (51), a question arises about the description of the several scales in cellular materials as synthetic materials become more and more complex in order to enhance their physical properties. The scales usually defined are thus presented in this section as well as the associated structural parameters.

Mesocellular foams

Scales description in foams When polymeric foams were first synthetically produced, their cell size was between 10^{-4} m and 10^{-2} m. They are today the more spread one. These foams with mesoscopic pores will now be referred to as *mesocellular foams*. The scales in cellular materials have been reflected from these mesocellular foams. In their review on the dynamic mechanical behaviour of foams (52), Sun et al. propose the following scales:

- Macroscopic scale (component) $> 10^{-1}$m
- Macroscopic scale (samples) 10^{-2}m - 10^{-1}m
- Mesoscopic scale (cellular structure) 10^{-4}m - 10^{-2}m
- Microscopic scale (base material) 10^{-6}m - 10^{-4}m
- Nanoscopic scale (base material highly porous) 10^{-9}m - 10^{-6}m

The above description is not suited for the microcellular and new nanocellular foams. This classical distinction between scales needs to be broadened to take into account the several types of cellular materials, from the mesocellular to the nanocellular.

Furthermore, new types of synthetic architected materials are being developed with multi-scales structurations (53; 54; 55; 56). A more general description inspired by the one used for natural materials with hierarchical structures (51) should allow an easier discussion and comparison between all those structured materials.

Cellular structure scale Foams are generally distinguished in two main categories based on their cellular structure: closed-cell foam and open-cell foams (6). In open-cell foams, edges form the cell network (fig. 2a). All the cells are interconnected and a fluid can flow through the cells.

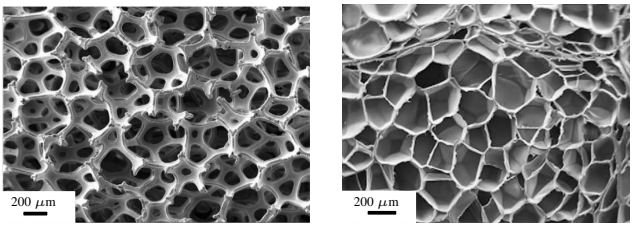

(a) Open-cell (b) Closed-cell

Figure 2. Differences between open (57) and closed-cell (58) foams and main features of these foams. Adapted with permission from Elsevier.

Foams with closed cells have well defined cells that are delimited by the cell walls. Between two cells, there are cell faces and at the junction of several faces are the cell edges (fig. 2b). The edges and the faces do not have the same thickness t_e and t_f respectively, especially in synthetic foams (6). ϕ is used to quantify the solid phase distribution (eq. 3). It represents the volume fraction of the solid contained in the edges of the cell (6). The remaining fraction $(1-\phi)$ is then in the faces.

$$\phi = \frac{t_e^2}{t_e^2 + \frac{Z_f}{\overline{n}} t_f l}, \tag{3}$$

where $\overline{n}$ is the average number of edges per face on a single cell and Z_f is the number of faces that meet on an edge. The thickness of the cell edges t_e and of the cell faces t_f are therefore also interesting structural parameters

to measure. To describe globally the cellular structure, three main parameters are used:

- the cell size d,
- the relative density ρ_r (eq. 1) or the expansion ratio X (eq. 2),
- the cell density N_c (eq. 4) defined as the number of cells per cubic centimetre of the unfoamed sample.

$$N_c = \left(\frac{n}{A}\right)^{3/2} \rho_r, \tag{4}$$

where n is the number of cells observed in an area A in cm^2. In addition, to refine the cellular structure description, other parameters and their distribution can be measured like the open-cell content (59).

Microcellular foams

Microcellular foams are characterised by cell sizes between 1 and 100 μm. More restrictive definitions place microcellular foams as foams with pores smaller than 10 μm (60) or smaller than 1 μm. The density of the cells varies from 10^6 to 10^9 cells/cm^3 in the Mucell process (22; 23; 61), which was one of the first process developed to produce microcellular polymeric foams. Many were developed after it, from batch foaming (rapid temperature rise and/or rapid pressure quench) to continuous extrusion foaming (25). These processes strongly dictate the resulting structure. Pang et al. reviewed in 2022 six resulting types of cell structures (60) depending on the evolution of the cell size, the cell density and the expansion ratio. It seems microcellular foams are mostly closed-cell (60), however open-cell microcellular foams have also been produced (62).

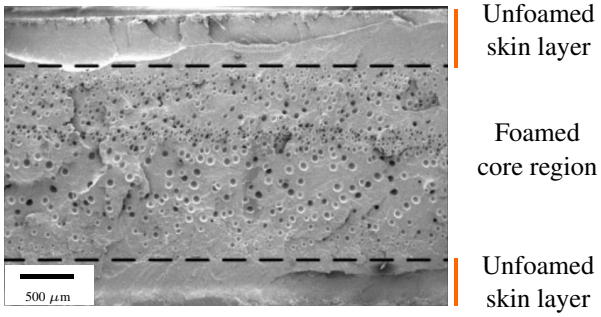

Figure 3. SEM image of the cross-section of microcellular injection-molded parts. Adapted from (63), courtesy of SAGE Publications.

Injection moulded foams have a solid skin on their surface (fig. 3). This is generally attributed to the rapid solidification of the polymer-gas solution attached to the cold wall of the mould cavity. In addition, the cell structure is not homogeneous and becomes increasingly deformed as one moves away from the injection site (64). Dong et al. explain these two phenomena by two mechanisms involved in the cell formation process: foaming during filling and foaming after filling (27; 63).

Nanocellular foams

As reported above, nanocellular foams that have been produced present a high relative density (0.21 - 0.81). An important work was made by Demewoz and Yeh to compute all research made on nanocellular foams and to obtain a visualisation of the relative density versus the cell size (fig. 4) (65).

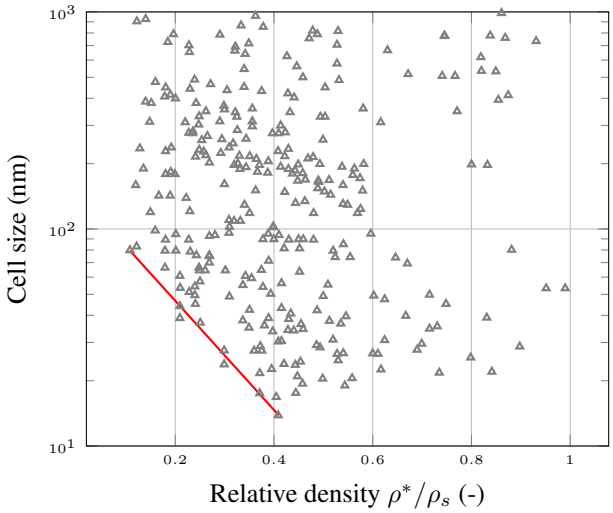

Figure 4. Overview of relative density versus cell size of nanocellular foams adapted from (65), courtesy of Elsevier (log-linear scale).

From this analysis, it appears that for now a physical limit exists. It seems complex to decrease the relative density and the cell size at the same time. This limit is represented by the red curve on the fig. 4. The nanocellular foam with the smallest cell size (13 nm) was produced by Martin-de-Leon et al. with a relative density of 0.41 (41). The nanocellular foam with the lowest relative density (0.18) was produced by Yeh et al. with a cell size of 65 nm (66). Both of these foams were obtained with PMMA.

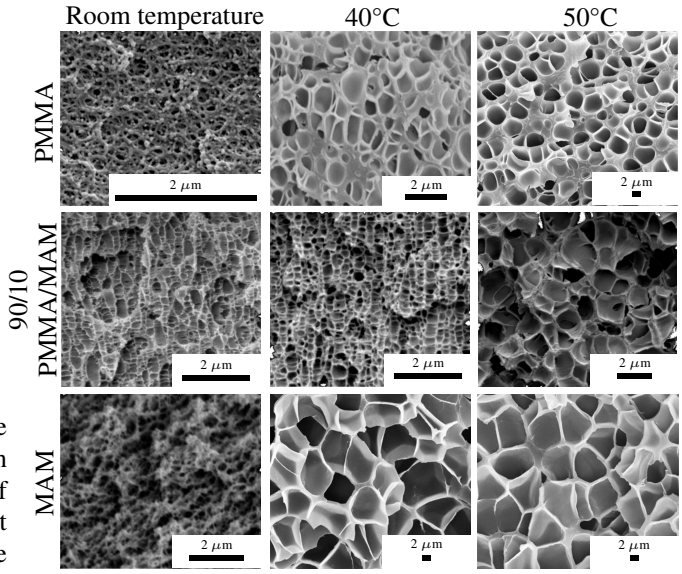

Figure 5. SEM pictures of the cellular structure of several foams produced in batch after CO_2 saturation at 30 MPa, at different temperatures from neat PMMA, 90/10 PMMA/MAM and neat MAM (PMMA-co-PBA-co-PMMA block copolymer). Adapted from (43), courtesy of Elsevier.

This highly impacts the typical nanocellular structure that can be observed through scanning electron microscopy

(SEM). Indeed, the majority of mesocellular foams and a few microcellulars foams present a relative density smaller that 0.1. On the contrary as shown by fig. 4, nanocellular foams demonstrate most of the time higher densities. The resulting structure of nanocellular foams is thus very different from meso and microcellular foams (see fig. 5). Nanocellular foams presenting the smallest cell size are open-cell (30) Furthermore, nanocellular foams display thick cell edges in comparison to their own cell size. On the contrary, low-density micro- and mesocellular foams can display very thin cells walls.

Beyond a qualitative description, determining the actual cell size of nanocellular polymeric foams presents significant challenges due to the inherent complexities of nanoscale structures and limitations of existing characterization techniques. Among the difficulties encountered in accurately determining the cell size of nanocellular foams lies the instrumentation limitations as SEM has resolution limitations that prevent accurate characterization of cell sizes below a certain threshold, typically around 50 nm. Sample preparation is also complex as porous structures are easily damaged during sample preparation, leading to inaccurate measurements. This could decrease the accuracy when analysing the effect of the cell size on the different physical properties of these foams. Nano-tomography could be a useful tool to obtain an accurate quantitative description with 3D informations (67; 68) as it was previously done on micro and mesocellular foams thanks to microtomography (69; 70; 71).

Finally, the typical nanocellular structure is today made of an unfoamed skin layer (72), like for the microcellular foams. Recently, the incorporation of a flexible gas diffusion barrier on the polymer surfaces during the saturation and foaming processes has nevertheless made it possible to considerably reduce this skin (73).

Compressive mechanical behaviour of foams

Typology

The mechanical behaviour of a cellular material is strongly dependent on its constitutive material and its relative density ρ_r (6). The classical mechanical behaviour of foams under compression display three phases: pseudo-linear elasticity, plateau and densification (fig. 6). Three distinct mechanical behaviours (elastomeric, elastoplastic and brittle) can be distinguished due to their plateau phase (fig. 6) (6). To these three behaviours (fig. 6), three types of deformation mechanisms have been associated (fig. 7), thus linking the behaviour of the structure at the macroscopic scale to that of the cell's deformation modes at a more local scale.

- For an elastomeric behaviour (75), the stress plateau is governed by the elastic buckling of cells starting at σ^*_{el} (fig. 7a). It is a non-linear elastic behaviour.
- An elasto-plastic foam has a stress plateau induced by the formation of plastic hinges during the buckling of its cell walls (76; 77) (fig. 7b). The plateau that starts at σ^*_{pl} can thus be referred to as a "plastic plateau".
- In elastic-brittle behaviour, the plateau stage is due to a succession of micro-cracks in the cells struts (fig. 7c) (78).

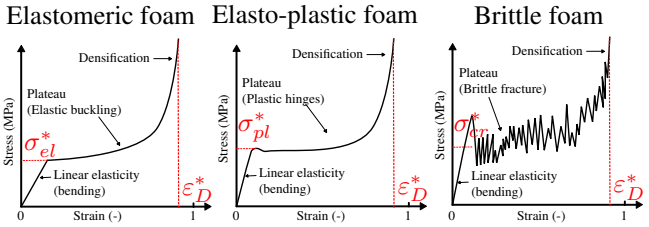

Figure 6. Stress-strain curves of different types of foam: elastomeric, elasto-plastic and brittle. Adapted from (74), courtesy of Elsevier.

The plateau phase of the macroscopic mechanical behaviour is then not as smooth as in the two previous cases (fig. 6).

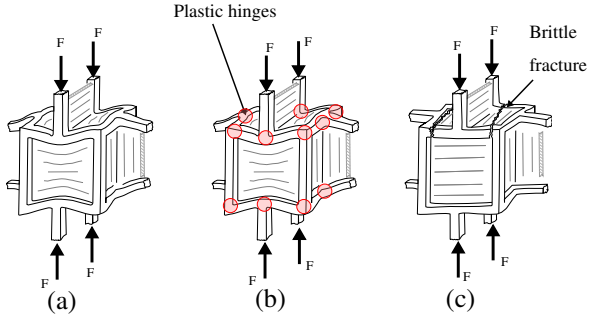

Figure 7. Deformation modes of closed cells, adapted from (74), courtesy of Elsevier. (a) Elastic buckling (b) Plastic buckling. (c) Brittle fracture.

Of these broad categories of mechanical behaviours, some behaviour can be hybrid. The deformation mechanisms are generally complex and difficult to unify behind a single definition in the case of nanocellular foams because the cellular structure and the constitutive materials vary from one study to another and have a great influence on these local mechanisms. Their identification can be done through various mechanical tests in parallel with *post-mortem* cellular structure observation (58) or an evolution of the cellular structure during a mechanical test (79; 80).

Associated models

Over the last 55 years, many mechanical models have been proposed to describe the mechanical behaviour of cellular materials. One of the most used model is the model developed by Gibson and Ashby based on a cubic cell with cell walls loaded in bending when macroscopically loaded in compression or tension (6) (fig. 7). This model and more globally its utilisation has been criticised since by Mills as it is important to keep in mind it is a semi-quantitative mechanics analogue for foam behaviour (81). Other models have been developed to propose a more accurate prediction of the mechanical behaviour based on the topology of the cell. A large part of them focuses on the first linear part of the curve (elastic moduli) and on open-cell foams. Few of them aim at predicting the mechanical behaviour until densification (82).

It has been shown in section 3 that a large variety of foam cells morphology exists between mesocellular, microcellular and nanocellular foams. The very accurate models relying on a precise cellular structure are then not suitable to compare

the mechanical behaviour of all these different foams. That is why the Gibson and Ashby model will be more deeply presented and used to discuss experimental results from different studies in the following review article.

Linear elasticity Under a compressive loading, the mechanical behaviour is first characterised by a pseudo-linear elasticity regime happening at small strains (see fig.6). For open cell foams, the only mechanism involved according to Gibson and Ashby is cell wall bending,

$$\frac{E^*}{E_s} \approx \left(\frac{\rho^*}{\rho_s}\right)^2, \tag{5}$$

with E_s, the Young's modulus of the constitutive material.

The calculation of the Young's modulus E^* of closed cell foams takes into account more mechanisms. In addition to bending, the faces are stretched and the fluid in the cells is compressed. Therefore, Young's modulus is a function of E_s, ρ^*, ρ_s, ϕ (eq. 3) and the Poisson's ratio of the foam ν^*:

$$\frac{E^*}{E_s} \approx \phi^2 \left(\frac{\rho^*}{\rho_s}\right)^2 + (1-\phi)\frac{\rho^*}{\rho_s} + \frac{\rho_0(1-2\nu^*)}{E_s(1-\rho^*/\rho_s)}. \tag{6}$$

Several extensions to Gibson and Ashby's model have been proposed over the years (83). Among them, we can note the one developed by Jo et al. (84). It has been shown that foams with a stretching dominated architecture have a different dependency to the relative density (85; 86),

$$\frac{E^*}{E_s} \approx \frac{\rho^*}{\rho_s}. \tag{7}$$

It follows that this kind of cellular structures with $\rho^*/\rho_s = 0.1$ is about ten times stiffer than a bending-dominated structure (86).

Buckling stress Many of the microcellular and nanocellular foams studied appear to be mainly foams with elasto-plastic behaviour. This means that when the macroscopic stress reaches the non-linear phase, plastic hinges appear when the cell walls deform non-linearly. The equation proposed by Gibson and Ashby to determine the buckling stress of elasto-plastic foams σ^*_{pl} is, for open cell foams,

$$\frac{\sigma^*_{pl}}{\sigma_{y_s}} \approx 0.23 \left(\frac{\rho^*}{\rho_s}\right)^{3/2} \left(1 + \left(\frac{\rho^*}{\rho_s}\right)^{1/2}\right), \tag{8}$$

with σ_{y_s}, the yield strength of the base material. This equation can also be used for closed cell foams, although a specific equation has been developed that takes the atmospheric pressure p_{at} and the inner pressure of the cells p_0 in to account,

$$\frac{\sigma^*_{pl}}{\sigma_{y_s}} \approx 0.3 \left(\phi\frac{\rho^*}{\rho_s}\right)^{3/2} + 0.4(1-\phi)\frac{\rho^*}{\rho_s} + \frac{p_0 - p_{at}}{\sigma_{y_s}}. \tag{9}$$

For elastomeric and brittle foams, expressions for buckling stress or collapse stress respectively, can also be obtained (6).

Densification The densification phase begins at ε_d when there is a generalisation of the contact between cell walls (87). Few models venture beyond the buckling stress. This is the case of Jo et al. (84), which proposes an expression from the Gibson and Ashby formalism to predict the strain at densification,

$$\varepsilon_d = \frac{s-\delta}{l} = \left(1 - \frac{t}{l}\right)^2 \left(1 + \frac{t}{l}\right), \tag{10}$$

with l and t corresponding to the characteristic size of the cell size and cell wall thickness respectively, s is the initial height of the cell without the cell walls and δ is the height of the cell when the two opposite walls are in contact.

Influence of cell size on the Young's modulus

The analytical models presented above where developed for mesocellular foams. They do not take into account the cell size. With the development of new manufacturing processes enabling the production of micro- and nanocellular foams, these models can be now compared with experimental data on these new foams. Results on micro- and nanocellular foams will be first presented, then an analysis of the experimental data gathered in these studies using the Gibson and Ashby models will be performed.

Tests performed and foams tested The mechanical behaviour of microcellular and nanocellular foams was mainly studied in compression, 3-point bending and tension. Several thermoplastic polymers were used to obtain microcellular foams (tab. 1). The majority of the polymeric microcellular foams are from thermoplastic amorphous polymers (polycarbonate (PC) (9), polyetherimide (PEI) (96), PMMA (91), acrylonitrile butadiene styrene (ABS) (64)). Only few semi-crystalline cellular polymers have yet been studied (low-density polyethylene (LDPE) (89)). The linear elastic mechanical behaviour of nanocellular polymeric foams has mainly been studied through PMMA-based systems (tab. 1). This is due to the fact the majority of nanocellular foams are made from PMMA as explained in section 2.

Young's modulus of microcellular foams For foams with a pore size around 15 μm, a significant density effect is unsurprisingly observed on PMMA microcellular foams tested in compression (98). A more interesting result shows that for a relative density of 0.05 and 0.033, foams with larger average cell size have worse mechanical properties (in terms of buckling stress and Young's modulus) than foams with smaller cells (98). The cell sizes studied ranged from 446 to 5.4 μm for the density of 0.05. For both densities studied, the modulus evolves according to a power law and the plateau stress increases linearly with decreasing cell size. The foam with cells around 446 μm displays a very different cellular structure with many defects in comparison to foams with cells below 200 μm. The cellular structure and the mechanical behaviour in compression are very similar for foams with cell size between 200 μm and 5.4 μm. Therefore, rather than a cell size effect, the decrease in Young's modulus with larger cells appears to be caused by the numerous defects.

Article	Material	Test	Dimensions mm or mm^3	Speed mm/min	Size (μm)	ρ^*/ρ_s (-)
Microcellular foams						
Kumar et al., 1994 (9)	PC	Tension	ASTM D638 (type IV and V)	10	1.6 - 8.9	0.1 - 0.97
Kumar et al., 1998 (88)	PVC	Tension	ASTM D638 (type IV)	10	x	0.28 - 1
Rodriguez-Perez et al., 2002 (89)	LDPE	Compression	Ø 0.1 × 11	60	312-956	0.05 - 0.03
Sun et al., 2002 (90)	PESF/PPSF	Compression	10 × 10 × 4	1	2-13	0.35-0.90
Fu et al., 2005 (91)	PMMA	Tension	1.5 to 3 (thickness)	1	7.6-11.7	0.23-0.72
Bureau et al., 2006 (92)	PC	Tension	ASTM D638 (type IV)	5	3-9	0.7-0.9
Nadella and Kumar, 2007 (93)	ABS	Tension	ASTM D638 (type IV)	10	x	0.35 - 0.8
Rodriguez-Perez et al., 2008 (94)	LDPE	Compression	Ø 22.8 × 17.5	1	30 - 100	0.27-0.92
Weller and Kumar, 2010 (95)	PC	Tension	ASTM D638 (type IV)	10	2.8 - 37.1	0.5
Miller et al., 2011 (96)	PEI	Tension	ASTM D638 (type IV)	10	2-4	0.75 - 0.9
Notario et al., 2015 (97)	PMMA	Tension	ISO 527-2	0.5	2.5 - 11	0.49-0.52
Gomez-Montverde et al., 2016 (64)	ABS	3 pt bending	100 × 10 × 5	10	5-47	0.77 - 0.93
Wang et al., 2017 (98)	PMMA	Compression	Ø 15×10	1	5-400	0.02-0.1
Wang et al., 2017 (21)	PMMA/TPU	Compression	Ø 8 ×10	0.8	0.9-4.6	0.09-0.11
Wang et al., 2019 (99)	TPU	Compression	8×8×8	1	4 - 80	0.08 - 0.5
Zhang et al., 2020 (100)	PMMA	Compression	5×5×5	0.5	2.4-52	0.14-0.74
Nanocellular foams						
Miller and Kumar, 2011 (96)	PEI	Tension	ASTM D638 (type IV)	10	0.03-0.12	0.75-0.9
Reglero Ruiz et al., 2011 (33)	PMMA-MAM	DMA bending	x	1 Hz	0.2-0.3	0.5-0.7
Pinto, 2014 (101)	PMMA	DMA bending	15×2×2	1 Hz	0.72-1.87	0.44-0.48
Pinto, 2014 (101)	PMMA-MAM	DMA bending	15×2×2	1 Hz	0.15-1	0.36-0.58
Notario et al., 2015 (97)	PMMA	Tension	ISO 527-2	0.5	0.2-0.6	0.42
Wang et al., 2017 (21)	PMMA/TPU	Compression	Ø 8 ×10	0.8	0.2	0.12
Martin-de-Leon et al., 2019 (19)	PMMA-MAM	Compression	10×10×4	5	0.02-0.08	0.37-0.53
Bernardo et al., 2019 (16)	PMMA-sep	Compression	10×10×4	5	0.3-0.5	0.27-0.53

Table 1. Assessment of the various experimental campaigns carried out on the mechanical behaviour of microcellular and nanocellular foams. x: when no mention of the given parameter was made in the article. Ø: indication of the diameter of a cylindrical test specimen.

This trend is also observed in the work of Zhang et al. for PMMA microcellular foams with a relative density around 0.08 and an average cell size between 15 and 45.7 μm (100). The plateau stress decreases slightly from 6.84 to 4.7 MPa with an increasing cell size (from 15 to 47 μm). For PC foams tested in tension, Young's modulus, elongation and stress at break do not appear to be dependent on cell size for foams with a relative density of 0.5 and cell sizes ranging from 2.8 to 37.1 μm (95). Relatively dense PEI microcellular foams have also been obtained (tab. 1) (96). In tension, an increase in stress and strain at break was observed for the PEI microcellular foams while the Young's modulus remained unchanged.

On the contrary, a work on thermoplastic polyurethane (TPU) microcellular foams (4-80 μm) reports an increase in plateau stress and Young's modulus with the increase of the cell size (from 8.8 to 68.8 μm) (99). Wang et al. commented on these results by mentioning the excessive stretching caused by foaming that can deteriorate the polymer matrix. Therefor, apart from this study, all the other results on microcellular polymeric foams seem to point to the fact that the Young's modulus is independent of the cell size below 100 μm.

Young's modulus of nanocellular foams The work of Martin-de-Leon et al. further demonstrates that this trend is true, even for nanocellular foams. The authors observe that for cell sizes between 4.3 μm and 20 nm at relative densities ranging from 0.2 to 0.51, the size of the cells at iso-density, whether micrometric or nanometric, does not influence the Young's modulus (19).

Three-point bending tests were realised by Reglero Ruiz et al. on nanocellular PMMA-MAM foams with a relative density from 0.4 to 0.7 and an average cell size of 200 nm (33). The storage modulus obtained varies between 0.5 and 1.2 GPa, and unsurprisingly increases with the density of the foam. They also tested the solid material using the same procedure and measured a storage of 3.4 GPa. For similar densities, Reglero Ruiz et al. claimed that Fu et al. found lower values for Young's modulus in pure PMMA microcellular foams (cell sizes between 8 and 15 μm) (91). However it seems that for relative densities around 0.4, the microcellular PMMA foams tested in tension by Fu et al. presented a Young's modulus between 0.5 and 0.3 GPa which is close to the values found for nanocellular foams by Reglero Ruiz et al.. The discrepancies could be explained by the different loading types (3 point bending versus tension) and the fact Dynamic Mechanical Analysis (DMA) allows to obtain the storage modulus which is not exactly similar to the Young's modulus.

The same authors carried out a further study on PMMA and PMMA10%MAM (101). 3-point bending tests with DMA were carried out at room temperature to measure the storage modulus. PMMA foams have a much lower storage modulus than PMMA10%MAM foams and the authors suggest that this difference may be due to the greater homogeneity of PMMA10%MAM foams. However, to reach this conclusion, they compare foams with similar cell sizes but different densities. For pore sizes between 150 and 1000 nm, they show that the storage modulus related to the square of the density seems almost stable. According to them, the modulus does not depend on the cell size in this range of cell sizes, contrary to what has been shown previously.

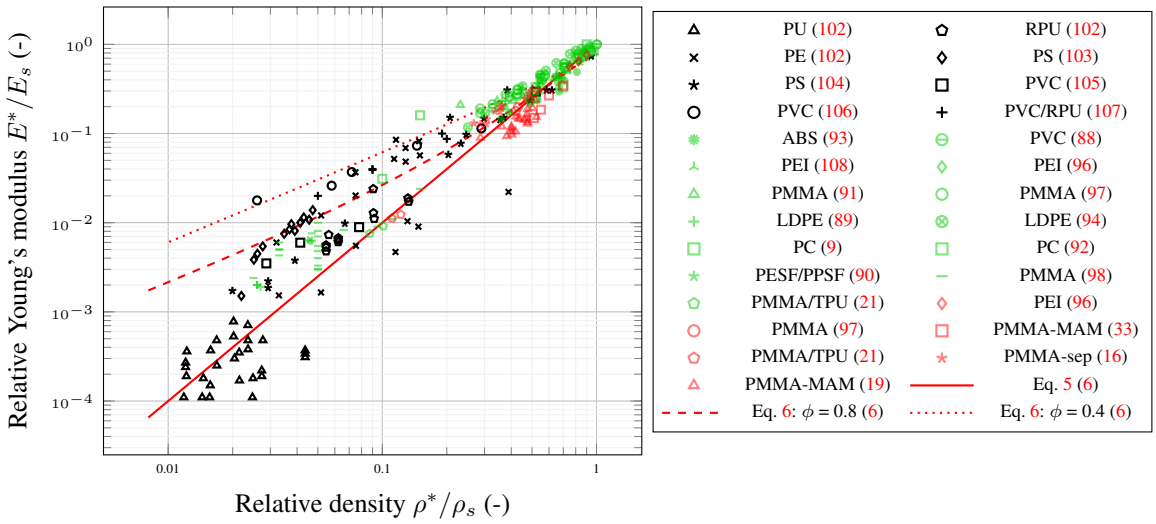

Figure 8. Relative Young's modulus plotted as a function of relative density for different foams. In black, mesocellular foams. In green, microcellular foams. In red, nanocellular foams (log-log scale).

Further analysis By placing these works and other ones in the perspective of relative density and constitutive materials, it is possible to plot the evolution of the relative Young's modulus as a function of relative density for a large number of polymeric foams (see fig. 8). The evolution predicted by the equations 5 and 6 obtained from Gibson and Ashby's analytical model based on PMMA values for closed cell foams are also plotted in this figure.

According to fig. 8, relative density appears to be the dominant factor in the evolution of the Young's modulus. Results on meso-, micro- and nanocellular foams all conform to the predictions of the Gibson and Ashby model, regardless of the cell size. Indeed, the Young's modulus values are mainly found between eq. 5 for open cell foams and eq. 6 for closed cell foams with $\phi = 0.8$. This is because most synthetic foams (even closed cell ones) behave as if they had open cells, as the surface tension draws much of the solid material into the cell edges during manufacture (109). This is the case for some of the PMMA foams studied by Wang et al. (98). The foam has a mechanical behaviour comparable to that of an open cell foam in terms of Young's modulus. However, SEM characterisation showed that it is a closed-cell foam.

Thus, it appears that there is no perceptible effect of the cell size on the Young's modulus of polymeric foams. However, the work of Wang et al. provides a contrast to this statement (98). For a similar relative density of microcellular PMMA foams, they were able to show that the modulus could vary according to the cell size. However, these values remain within the spectrum predicted by the Gibson and Ashby model. In order to refine these results, it would be necessary for each foam of the same relative density to establish the degree of closure of the cell walls from a mechanical point of view. Fig. 8 and tab. 1 also show that few results are currently available on the Young's modulus of nanocellular foams. Moreover, those that are produced have a high relative density, between 0.12 and 0.9.

Influence of the cell size on the buckling stress

In contrast to the linear elastic part, the buckling stress can be associated with different deformation mechanisms (elastic buckling, elastic buckling and plastic hinges, cracking) (6). In this section, we focus on polymeric foams with elasto-plastic mechanical behaviour in compression. The appearance of plastic hinges during cell wall buckling is the main deformation mechanism in elasto-plastic foams, particularly PMMA. It is mainly for this type of foams that nanoscopic porosities have been obtained.

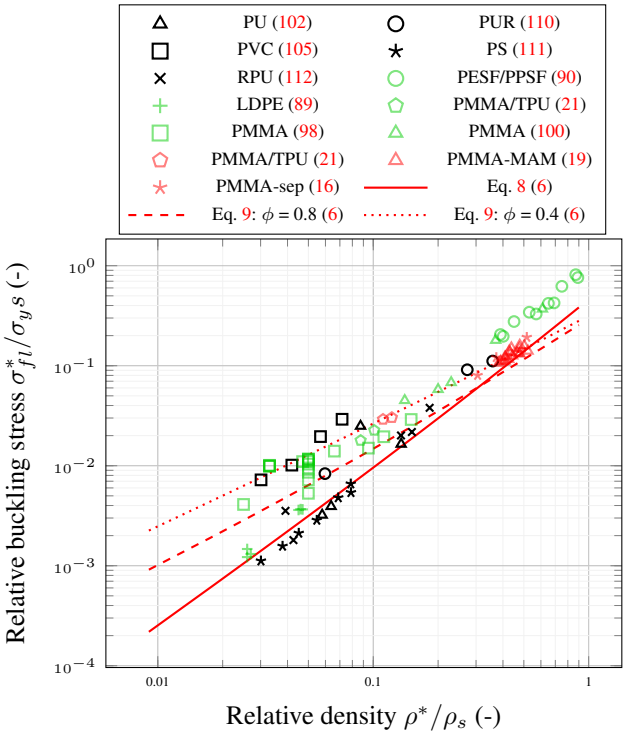

Figure 9. Relative buckling stress from compression tests as a function of relative density of different foams compared to the prediction given by the Gibson and Ashby model. In black, mesocellular foams. In green, microcellular foams. In red, nanocellular foams (log-log scale).

Buckling stress of micro and nanocellular foams Compared to Young's modulus, fewer results are available on the buckling stress of elasto-plastic foams, both for microcellular and nanocellular foams. Indeed, only compression tests can allow to obtained this parameter unlike DMA or quasi-static tensile tests. As with Young's modulus, Wang et al. show that at very low relative densities (0.05 and 0.033), as the cell size increases in microcellular PMMA foams (from 5 to 550 μm), the buckling stress decreases (98). But here too, the values remain within the spectrum of properties predicted by the Gibson and Ashby model. Furthermore, Martin-de-Leon et al. demonstrated that for PMMA micro- and nanocellular foams, the size of the cells does not influence the buckling stress (19).

Otherwise, all the other studies made on microcellular and nanocellular foams have been made on foams with different densities and different cell sizes. It is thus complex to decorrelate both effects on the buckling stress with these sole results by considering one study at the time.

Further analysis As with the Young's modulus, the different values of buckling stresses were listed and divided by the value of the yield strength of the constitutive material σ_{y_s}. The values obtained were then plotted in fig. 9 as a function of the relative density of the different foams.

Concerning the buckling stress, the relative density is also a preponderant factor to be taken into account (fig 9). The buckling stress increases with density following a power law predicted by the Gibson and Ashby model. Depending on whether the material has open or closed cells, this law varies (eq. 8 and 9). It appears that microcellular PESF and PPSF foams studied by Sun et al (90) present a higher buckling stress than what the Gibson and Ashby model predicts (fig. 9). However no explanation of such behaviour could be given. Nevertheless, these results on PESF/PPSF microcellular foams must be considered carefully, as two or three parts were glued together to obtain a specimen for compression tests.

The majority of the foams tested seem to behave either as open foams or as foams with ϕ within the range [0.4,1]. Thus, contrary to the evolution of the relative Young's modulus with density (fig. 8), the buckling stress of the closed foams really seems to follow the law expected for these foams. Furthermore, it appears that the compressive behaviour has mainly been studied for low strains and at low strain rates. It could be interesting to further investigate the mechanical behaviour of nanocellular foams by looking at their mechanical behaviour until densification.

Brief summary of the compressive properties

With regard to the influence of cell size on the compressive properties, it would appear that current knowledge shows that under quasi-static loadings and for small strains, a reduction in cell size has no noticeable effect. Under quasi-static conditions, compression and tension tests were mainly performed on microcellular foams while DMA 3 point bending tests were also performed in addition to tension and compression on nanocellular foams. It explains why many data exist on the Young's modulus (fig. 8) while it is more scarce for the buckling stress (fig. 9).

Furthermore, direct comparison of the mechanical behaviour of meso-, micro-, and nanocellular foams, has been difficult since data at a given foam density is hardly available. As displayed on fig. 8 and fig. 9, mesocellular foams often present a relative density below 0.1, while microcellular and nanocellular foams generally have a relative density of 0.2 and above. That is why analytical models were used to try to dissociate the influence of the relative density and the influence of the cell size.

To complete this analysis on the influence of the cell size on the compressive behaviour of polymeric foams, the following research directions are the main ones to follow:
- Influence of the cell size on the mechanical behaviour at large strains by performing compressive tests until at least a nominal strain of 0.7 and by measuring the parameters associated with the plateau and the densification;
- Influence of cell size coupled with crystallinity by mechanically testing, along with amorphous foams, semi-crystalline foams with different cell sizes and relative densities;
- Influence of the cell size coupled with the influence of the strain-rate by considering a larger range of strain-rates as done by Zhang et al. (113).

Fracture properties of foams

In tension, the deformation mechanisms are very different from those in compression presented above (6). Failure mechanisms occur in all cellular materials above a certain tensile strain. However, the fracture behaviour of cellular polymeric materials remains complex to understand for two main reasons: the effect of the architecture and the nature of the material (*i.e.* polymer). The effect of the cell 3D architecture is not well documented in the literature and this makes it difficult to apply fracture mechanics formalisms suitable for homogeneous materials (114; 115). It is difficult to define which fracture mechanics formalism, LEFM (**L**inear **E**lastic **F**racture **M**echanics) or EPFM (**E**lastic **P**lastic **F**racture **M**echanics), to apply depending on the size of the **F**racture **P**rocess **Z**one (FPZ). The focus is more on the emergent behaviour of the material, brittle or ductile. Depending on the microstructure, the fracture surface is also complex to estimate. The projected area (the thickness of the specimen multiplied by the length of the crack) is generally considered. The organic nature of the material makes it necessary to describe the evolution of the fracture properties as a function of the visco-elastic plastic behaviour. Indeed, the fracture properties of polymers are strongly dependent on certain conditions (environment, strain rate, stresses, manufacturing process, etc.) which may affect the rheological behaviour of the polymer. A polymer that is ductile at intermediate temperatures and velocities can become brittle at low temperatures or high velocities (116).

To describe the evolution of the fracture properties of polymers, and their dependence on rheological properties, kinetic laws of fracture are usually established (117; 118; 119; 120). The latter must show the evolution of a fracture parameter, such as fracture toughness or fracture energy, as a function of the cracking regime, i.e. the cracking velocity. The results described in the literature for cellular materials have little relation to cracking kinetics. This is also partly

true for dense polymers. It is therefore sometimes difficult to conclude on a potential effect of the microstructure. Nevertheless, the objective here is to review the knowledge of fracture in cellular polymer materials and to define the potential limitations to be overcome in order to conclude on an effect of microstructure on fracture properties. Small-scale architecture of structured materials could lead to substantial mass savings (121) or the achievement of much higher fracture properties at iso-density. Since the 1980s, the fracture properties of foams have been studied for various constitutive materials: Rigid polyurethane (RPU) (122; 123; 107), poly(vinyl chloride) (PVC) (124; 125), polystyrene (126), ABS (64), PMMA (19) and PC (92). There now seems to be a greater interest in unifying all the results and models generated so far (127).

Typology and associated models

As with dense materials, the two main fracture behaviours are categorised as brittle and ductile. In most cases, the fracture response of the specimen is primarily driven by the fracture behaviour of the dense material. Although changing the microstructure of brittle polymers (from dense to cellular) can change the fracture response to quasi-brittle or ductile (108; 96). In 2016, Gomez-Monterde et al. found that the mechanical fracture behaviour of ductile polymer foams had been little studied (64). At the time, most work focused on rigid and brittle polymeric foams such as RPU or PVC foams (127). These materials have a linear elastic fracture behaviour that can be analysed by the LEFM formalism.

Brittle foams When a brittle foam is loaded in tension, the edges of the cells deform elastically. The load is transmitted through the foam as a set of discrete forces and moments acting on the cell edges. Crack advancement can occur in two ways: by flexural failure of the non-vertical cell walls or edges (fig. 10a), or by failure of the vertical elements under a combined tensile and bending moment (fig. 10b) (128). *In situ* observations under SEM showed that in PVC foams, it was the tensile mechanism of the vertical walls that was mainly responsible for the cracking (125).

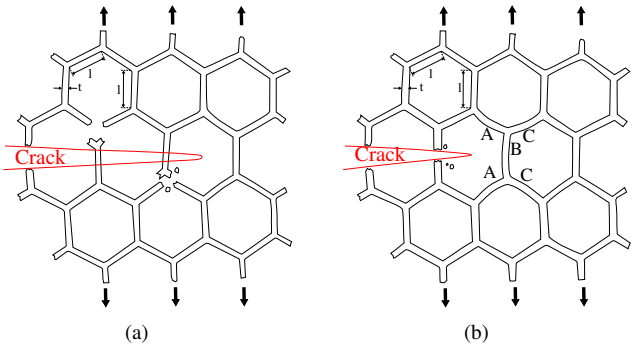

Figure 10. Failure mechanisms in brittle foams, adapted from (109), courtesy of Elsevier.

At the scale of the cell size, the crack in a brittle foam therefore extends discretely (109). Each step advances the crack by one cell width. When considering brittle materials, the formalism of LEFM can be applied. The crack advance can be described according to the local (Irwin) and global (Griffith) approaches. The first one requires the stress intensity factor K_I to be higher than the fracture toughness ($K_I > K_{Ic}$). The second requires the energy release rate G_I to be greater than the fracture energy of the material ($G_I > G_{Ic}$). Since the foam is linear-elastic until the cell edges crack, the average force and moment on a given cell edge can be calculated from the stress field in the equivalent linear elasticity model.

The discrete problem can be solved by taking the solution of the equivalent continuous problem (anything done on a smaller scale by replacing the discrete bonds between the atoms with a continuous medium) and using it to calculate the forces and moments on the discrete cell edges. In tests on open-cell glassy carbon foams, Huang et al. showed that this assumption was valid for brittle foams when the ratio a/l, of crack length a to cell size l, was greater than 10 (129). A crack of length a in an infinite elastic solid, located perpendicular to a distant tensile stress σ^∞ creates a singular stress field:

$$\sigma = \frac{K_I}{\sqrt{2\pi r}} = \frac{\sigma^\infty \sqrt{\pi a}}{\sqrt{2\pi r}}, \tag{11}$$

at a distance r from its tip. Edges A and C in fig. 10 are then in bending while edge B is in tension. The following expression is then obtained, by linking relative density and microstructural parameters,

$$K^*_{Ic} = C_1 \sigma_f \sqrt{\pi l} \left(\frac{\rho^*}{\rho_s}\right)^{3/2}, \tag{12}$$

for an open cell foam, with l, the average cell size and σ_f, the stress at break of the base material. Whereas for a closed cell foam,

$$K^*_{Ic} = C_2 \sigma_f \sqrt{\pi l} \left(\frac{\rho^*}{\rho_s}\right)^{2}, \tag{13}$$

C_1 and C_2 being constants close to 1. Two strong assumptions discussed by Huang and Gibson (129) are made here:

- the length of the crack is much greater than the size of the cells,
- the stress at break of the cell wall σ_f is constant (defects are therefore not taken into account).

Ductile foams When the linear elastic assumption cannot be applied, *i.e.* when the material exhibits ductile behaviour and the size of the FPZ is large relative to the crack length, the EPFM framework is used. The fracture properties are usually evaluated by the parameters J-integral and **C**rack **T**ip **O**pening **D**isplacement (CTOD) (64).

The mechanical fracture behaviour of elasto-plastic and therefore ductile foams has mainly been studied in the context of metallic foams (130; 131; 132; 131; 133; 134; 135; 136; 79; 137) over the last decade. For highly ductile polymers (in the context of post-strain fracture mechanics), the effective work of fracture concept is the most common fracture characterisation technique. However, there is little research determining these parameters for cellular materials, such as PP foams.

As far as nanocellular foams are concerned, they have mainly been obtained with PMMA. PMMA is well known in the literature to be the elastic and brittle model polymer. The mechanical behaviour of PMMA nanocellular foams seems to be mainly brittle in tension. This review will therefore focus on this brittle behaviour with limited plastic visco-elastic effects compared to other polymers. The dependence on cracking kinetics will therefore not be discussed.

Test methods

Different types of tests can be carried out to assess the fracture conditions of cellular polymers. The main tests performed are tensile tests (122; 123), impact tests (such as Charpy and Gardner, described in section 6) and more specific fracture tests.

The fracture properties are mainly studied in the opening mode (mode I) because of its criticality. Indeed, the value of the fracture energy G_{Ic} is lower than in the other two modes (II and III). To construct the kinetic law of fracture in polymers, it is convenient to try to dissociate the resistance to initiation (or slow propagation) and fast propagation (when the material is brittle). Generally, initiation conditions are studied by monotonic or cyclic quasi-static tests for cracks of a few mm or even cm on notched specimens (fig. 11) such as compact tension (138), **S**ingle **E**dge **N**otched **T**ension (SENT) or **B**ending (SENB) (109; 107; 64; 19) and **D**ouble **E**dge **N**otched **T**ension (DENT) (139; 140). These types of configurations and stresses allow the study of resistance to fracture initiation (from brittle to ductile) through the calculation of the critical stress intensity factor K_{Ic} before failure. For these specific fracture specimen geometries, analytical solutions of K_{Ic} can be found in books on fracture mechanics (141). The resistance to fast propagation is related to the weakest fracture behaviour of the polymer (brittle). This behaviour is generally considered as the critical behaviour in design. The conditions for fast propagation require monitoring the progress of the crack over a few tens of cm. For that, the geometry of the strip band specimen was developed to impose a controlled load throughout the crack propagation. This configuration is widely known in the polymer community (142; 118; 119) but still little used for cellular materials (138). In the context of nanocellular foams, the first difficulty in carrying out all these tests is to obtain a specimen large enough to be tested on conventional test equipment. If this is not possible, then the use of micro-machines must be considered.

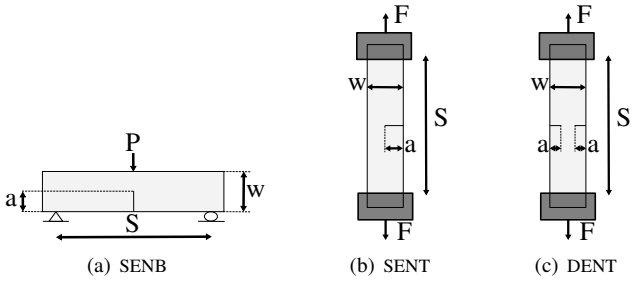

(a) SENB (b) SENT (c) DENT

Figure 11. Diagram of mode I fracture test specimens with different notched geometries. SENB: Single Edge Notched Bending. SENT: Single Edge Notched Tension. DENT: Double Edge Notched Tension.

The Weibull modulus can also be used to account for the probability of failure of a material under non-uniform loading. Weibull analysis predicts that brittle solids exhibit a "size effect" (larger specimens are weaker in tension) which depends on the Weibull modulus of the material. The probability of failure P_f for each cell wall under tension with a volume V equal to the volume of a single cell wall (129) is

$$P_f = 1 - exp\left[-\frac{V}{2(m+1)^2}\left(\frac{K_{IC}}{K_0}\right)^m\right]. \quad (14)$$

Using the Weibull distribution to account for variability in cell wall strength leads to a "cell size effect" which again depends on the Weibull modulus of the cell wall material.

Influence of cell size on fracture properties

Density effect Many studies have focused on the mechanical behaviour at failure of a specific material such as PU foams (140; 122) or PC (92). There are some studies that focus on the influence of density on the mechanical fracture behaviour of foams. Amongst them is the work of McIntyre who studied the fracture behaviour of PU foams (123). He noted that, as with other macroscopic material parameters, toughness increases with density.

The fracture behaviour of ABS microcellular foams was also studied in the quasi-static regime using the CTOD (64). For this purpose SENB specimens were used. The authors showed that, as expected, the cells act as crack stops by blunting the crack tip. Thus, the onset of crack propagation is delayed and a higher CTOD value is obtained for the less dense materials.

Non-polymeric foams There is a limited amount of research into the influence of cell size on mechanical behaviour. Some work, rather focused on ceramic foams, has shown that the toughness of brittle foams is sensitive to edge strength which, according to Weibull analysis, depends on cell size (143; 144; 145; 146; 147). Brezny and Green studied brittle reticulated vitreous carbon and showed that toughness is independent of cell size in the absence of microstructural change (146). Huang and Gibson extended this analysis by comparing glassy carbon foams of similar density at different l_1 and l_2 cell sizes (129). From the analytical expression of the stress intensity factor taking into account the Weibull modulus m,

$$K^*_{Ic,1}/K^*_{Ic,2} = \left(\frac{l_1}{l_2}\right)^{1/2-3/m}, \quad (15)$$

and 3-point notched bending tests, they show that the dependence of toughness on cell size is a function of the Weibull modulus of the cell wall material (129).

Polymeric foams Miller and Kumar compared the mechanical properties of microcellular (cell size in the range 2-5 μm) and nanocellular (cell size in the range 50-100 nm) PEI foams produced by CO_2 gas dissolution foaming, over a range of relative densities between 0.75 and 0.9 (96). Under tensile testing (148), they found that the nanocellular foams exhibited significantly higher strain-to-failure, with an improvement in modulus of toughness of up to 350% compared to microcellular foams.

In these tests, toughness is calculated by integrating the stress-strain curve. This is a macroscopic measurement that can make it difficult to separate the fracture properties from the overall response of the material. For example, for PC foams, Kumar and Weller did not observe any cell size effect when considering the tensile behaviour of microcellular PC foams and their toughness (ρ_r= 0.57, cell size between 2 and 37 μm]) (149). Bureau and Kumar later performed fracture tests on microcellular PC foams having a relative density of 0.7 and 0.9 and a cell size between 3 and 9μm (92). They used the compact tension specimen geometry coupled with the CTOD method. They were able to show that the fracture toughness of microcellular foams could be greater than the fracture toughness of the dense material. They observed that fracture in the studied foams occurs through the multiple initiation, growth and coalescence of voids formed at the cell level (92). The latter act as stress concentrators. According to them, a fine cell morphology would allow the growth and coalescence phases to be prolonged, and would thus improve the resistance to fracture.

To allow a quantitative comparison and to highlight cell size effect, specific fracture tests and specimen geometries need to be used like the compact tension specimen or SENT/SENB specimens. As mentioned in the section Test Method, the critical stress intensity factor K_{Ic}, also called the fracture toughness, is then calculated to study the resistance to fracture initiation. For meso, micro and nanocellular polymers, it was mostly determined using 3-point bending tests on notched specimens (SENB as detailed in tab. 2) (19). Some research focused on the effect of sample size or loading conditions on the fracture toughness of mesocellular polymeric foams (150; 151; 152). Others already focused on the effect of the cell size on the fracture properties of polymeric foams (153; 154; 155). Thus, Poapongsakorn et al. performed 3-point and 4-point bending tests on PVC foam notched specimens with a relative density around 0.043 with different cell sizes (0.57 to 1.71 mm) (153). They saw no effect of cell size on the failure behaviour of these brittle foams. The majority of these studies were performed before the advent of nanocellular foams. It is therefore proposed in this paper to update these analyses by comparing results from mesocellular, microcellular and nanocellular foams.

Further analysis Several researchers have compiled the results of the different fracture properties of different cellular materials. Thus, Jelitto and Schneider propose in 2019 to plot K^*_{Ic}/K_{Ic_s} as a function of porosity P (P = 1 - ρ^*/ρ_s) (158), focusing mainly on porous metallic materials. However, this does not seem to give access to a general law to study these properties (159; 160). Marsavina and Linul focused on the fracture toughness of rigid polymeric foams and on the influencing parameters (e.g., specimen type, solid material, density and loading speed) (127).

In the current review article, polymeric foams are also looked at, but focusing on meso-, micro- and nanocellular foams (tab. 2). The ratio K^*_{Ic}/K_{Ic_s} is here plotted against the relative density (fig. 12).

Taking the analytical expression of K^*_{Ic} given by Maiti et al. (109), we obtain for an open cell foam,

$$K^*_{Ic}/K_{Ic_s} = C_1\sqrt{l/a}\left(\frac{\rho^*}{\rho_s}\right)^{3/2}, \qquad (16)$$

with the main inputs being the density of the foam and the constitutive material, as well as the average cell size l and the pre-crack size a for the constitutive material. Similar correlations have been found in other works (161; 162)

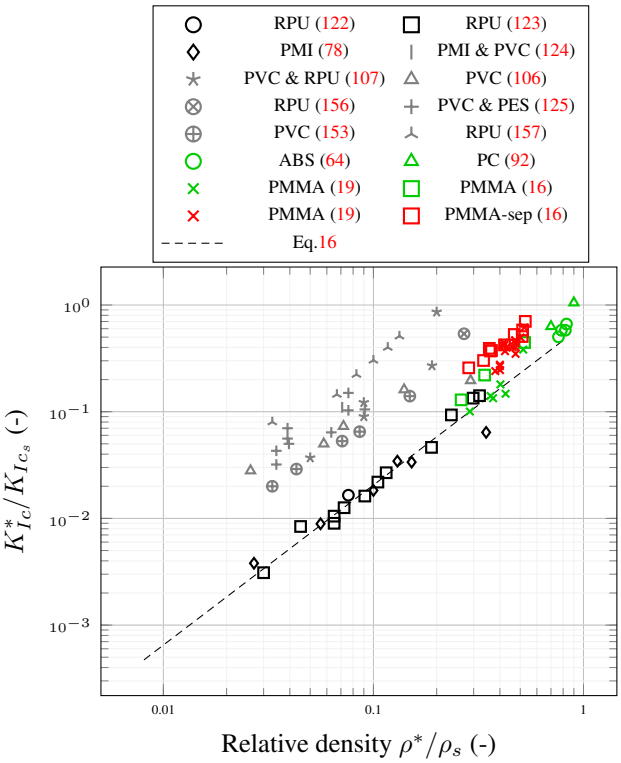

Figure 12. Relative K_{Ic} of different foams as a function of relative density, obtained mainly by 3-point bending and SENB specimens. In black and gray, mesocellular foams (with open and closed cells respectively). In green, microcellular foams. In red, nanocellular foams (log-log scale).

From the fig. 12, different trends can be observed. The results on which the model provided by Maiti et al. (109) were based are displayed in black and follow the eq. 16. More recent studies on mesocellular polymeric foams are displayed in grey. A better mechanical behaviour than the one predicted by eq. 16 is observed on fig. 12 for mesocellular PVC and RPU foams. The main difference is that all of these foams are closed-cells while all the black ones are open-cells. Therefore, like for the other parameters (e.g., Young's modulus and buckling stress), closed-cell foams demonstrate a greater fracture toughness.

The few studies carried out on the fracture behaviour of microcellular and nanocellular polymeric foams have been carried out on ABS, PC and PMMA foams (tab. 2). The fig. 12 does not show a clear effect of the cell size between micro and nanocellular PMMA foams. It seems that the eq. 16 proposed Maiti is relevant for most of microcellular foams (92; 64; 19). However the PMMA foams with a cell size under 1 μm demonstrate a higher toughness than expected (16; 19). PMMA-sep foams display an open-cell content between 0.030 and 0.070, it is therefore almost a full closed cell foam. It could therefore explain why values are higher than expected. For PMMA foams, microcellular

Article	Base material	Test	Dim. (mm^3)	a/l	Speed (mm/min)	Cell size	ρ^*/ρ_s (-)
Mesocellular foams							
Fowlkes, 1974 (122)	RPU	SENB/DENT/DCB	12.5×16.5×143	12.5 - 50	1.3	250 - 1000 μm	0.076
Mc Intyre et al, 1979 (123)	RPU	SENT	5×35×150	2 - 26	25	58 - 384 μm	0.02 - 0.33
Maiti et al., 1984 (109)	PMI	SENB	25×50×250	42	0.02-0.08	300 μm	0.03 - 0.15
Burman et al, 1998 (124)	PMI	SENB	5×35×150	x	25	500 - 700 μm	0.04
Burman et al, 1998 (124)	PVC	SENB	5×35×150	x	25	350 - 450 μm	0.08
Viana et al, 2002 (106)	PVC	SENB	12.7×25.5×108	28 -80	0.2	200 - 700 μm	0.03 - 0.3
Kabir et al., 2006 (107)	PVC	SENB	25×12.5×100	20	1.5	200 - 500 μm	0.05 - 0.2
Kabir et al., 2006 (107)	RPU	SENB	25×12.5×100	100	1.5	100 μm	0.2
Jin et al, 2007 (156)	RPU	SENB/SENT	5×35×150	76	1.5	150 μm	0.27
Saenz et al, 2011 (125)	PVC	SENB/DCB	13.9×25.4×127	15 - 30	12.7	440 - 840 μm	0.03-0.08
Saenz et al, 2011 (125)	PES	DCB	13.9×25.4×127	15 - 30	12.7	440 - 760 μm	0.04-0.09
Poapongsakor et al., 2013 (153)	PVC	SENB	13.5×25.4×101.6	15 - 38	12.7	330 - 840 μm	0.03 - 0.15
Marsavina et al, 2013 (157)	RPU	SENB	13×25×100	$\geq$ 50	2	50 - 200 μm	0.03 - 0.13
Microcellular foams							
Bureau et al., 2006 (92)	PC	CT	50×50×3	1200	10	3 - 9 μm	0.7 - 0.9
Gomez-Montverde et al., 2016 (64)	ABS	SENB	100×50×5	106	16	5 - 47 μm	0.77-0.93
Martin-de-Leon et al., 2019 (19)	PMMA	SENB	4×13.6×60	x	10	1 μm	0.29 - 0.35
Bernardo et al. 2019 (16)	PMMA	SENB	5×15×55	x	10	3 - 4.3 μm	0.29-0.52
Nanocellular foams							
Martin-de-Leon et al., 2019 (19)	PMMA	SENB	4×13.6×60	x	10	20-84 nm	0.37 - 0.53
Bernardo et al. 2019 (16)	PMMA-sep.	SENB	5×15×55	x	10	300 nm - 4.3 μm	0.27-0.52

Table 2. Summary of the different experimental campaigns carried out on the mechanical behaviour at breakage of foams. x: when the real length of the pre-crack was not indicated.

foams are predominantly closed cells while the nanocellular foams have open cells (19). It means that the PMMA nanocellular foams display a greater fracture toughness than closed-cell PMMA microcellular foams, even if they have open cells. It would therefore indicate a cell size effect when considering fracture properties.

One can also consider the experimental data using a different expression of K_{Ic}. The parameter $\overline{K_{Ic}}$, was indeed proposed by Maiti et al. (109),

$$\overline{K_{Ic}} = \frac{K^*_{Ic}}{\sigma_{f_s}\sqrt{\pi l}}. \tag{17}$$

The term $\sigma_{f_s}\sqrt{\pi l}$ is equivalent to the K_{Ic} of the solid material with a crack length l equivalent to the size of a cell. According to the analytical expression of K^*_{Ic} given in eq. 16, we then have for an open cell foam, an expression which only depends on the ratio of the relative densities,

$$\overline{K_{Ic}} = C_1 \left(\frac{\rho^*}{\rho_s}\right)^{3/2}. \tag{18}$$

Martin-de-Leon et al. have plotted $\overline{K_{Ic}}$ as a function of the relative density (19). Contrary to the material parameters related to the macroscopic compression behaviour (e.g., Young's modulus, buckling stress), they showed in this way an important effect of the cell size reduction on the macroscopic fracture behaviour. As the cell size decreases, the toughness increases. Additional data have been added to this figure from experimental results in the literature (tab.2). For micro and nanocellular PMMA foams, it was calculated using the tensile fracture strength found by Notario et al. on dense PMMA, $\sigma_{f_s} = 65\ MPa$ (97). A more complete figure is therefore proposed in fig. 13. It presents values of $\overline{K_{Ic}}$ as a function of relative density for different polymer foams, the same as those presented in fig. 12.

Mesocellular foams have a $\overline{K_{Ic}}$ between 3 10^{-3} and 4 10^{-1} (fig. 13). Like in fig. 12, there are two groups among

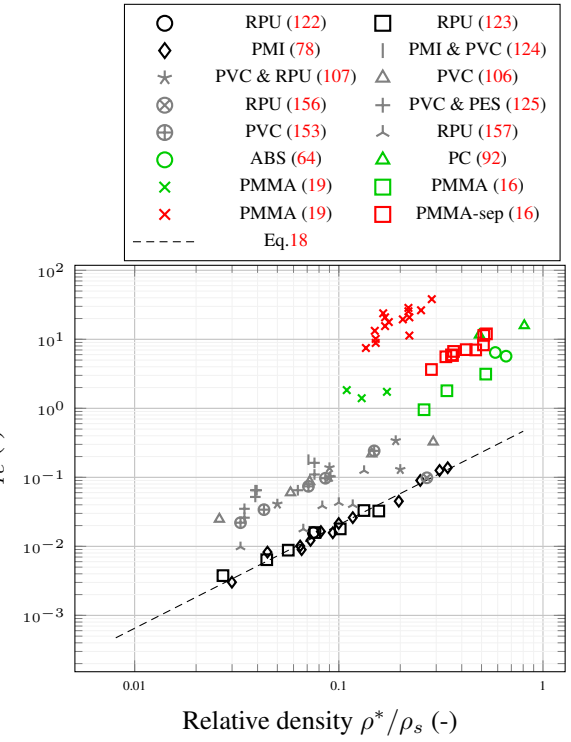

Figure 13. $\overline{K_{Ic}}$ of different foams as a function of relative density, obtained mainly by 3-point bending and SENB specimens. In black and gray, mesocellular foams (with open and closed cells respectively). In green, microcellular foams. In red, nanocellular foams (log-log scale).

mesocellular foams: open-cell foams in black and closed-cell foams in gray. The first one follows the equation proposed by Maiti et al. for open-cell foams (eq. 18). RPU closed-cell foams seem however also to follow eq. 18 while the other closed-cell foams with different constitutive materials do not. All these foams have similar cell sizes between 50 and 1000 μm. This parameter seems then to be material-dependant

which limits the comparison between a large number of studies on polymeric foams.

For microcellular and nanocellular foams, $\overline{K_{Ic}}$ is greater than 1 (fig. 13). $\overline{K_{Ic}}$ of PC, ABS and PMMA microcellular foams ranges from 7 10^{-1} to 2 10^{1}. $\overline{K_{Ic}}$ of microcellular foams seems to follow the same trend as that of mesocellular foams within a multiplicative factor. It could be due to the constitutive material itself as discrepancies are also observed between mesocellular foams. For nanocellular foams, made only of PMMA like the majority of microcellular foams, $\overline{K_{Ic}}$ is between 10^{0} and 5 10^{1}. It is then greater than $\overline{K_{Ic}}$ of microcellular foams while the only parameters that vary are the cell size and the cell type (open or close). Indeed, micro and nanocellular foams both made of PMMA have been studied.

With this data representation, the results obtained by Martin-de-Leon et al and Bernardo et al. on microcellular and nanocellular PMMA foams show an important increase in the toughness with the cell size reduction (19; 16). According to Bureau and Kumar, cells act as stress concentrates at the crack tip due to the triaxiality of the stress (92). In foams with smaller cells, the growth and coalescence phase of cracks would then be prolonged, which would explain this increase. However if one take a closer look at the experimental data, micro and nanocellular PMMA foams demonstrate a similar K^*_{Ic} (fig. 12). The calculation of $\overline{K_{Ic}}$ artificially increases the value of this parameter for nanocellular foams. $\overline{K_{Ic}}$ is divided by the root square of the cell size so the $\overline{K_{Ic}}$ of nanocellular foams is multiplied 32 times more than the $\overline{K_{Ic}}$ of microcellular foams. This represents more than the gap of value between the micro and nanocellular foams.

Brief summary of the fracture properties

Unlike other material parameters, the fracture toughness of foams has been less studied and theorised. Under quasi-static conditions, 3-point bending tests were mainly performed on notched specimens. These tests were always performed at a crack length well above the cell size to prevent any crack length effect.

However, there are discrepancies between studies that are difficult to interpret. Using K^*_{Ic} values obtained from these tests do not allow to draw any conclusion on the cell size effect on the fracture properties. Only a small cell size effect is observed when one plots the foam fracture toughness K^*_{Ic} against the base material toughness $K_{Ic,s}$ as a function of relative density. On the contrary, the plot of $\overline{K_{Ic}}$ as a function of relative density could show the interest of decreasing the cell size to increase the fracture performance of foams.

Therefore, depending on how the data is plotted, an effect of the cell size on fracture properties appears more or less clearly. Maiti et al., when proposing the calculation of $\overline{K_{Ic}}$, wanted to propose a normalised parameter as for the other material parameters. However, by considering only mesocellular foams, apart from a size effect, a purely material effect seems to emerge (fig. 13). Although a difference in $\overline{K_{Ic}}$ exists between the microcellular and nanocellular PMMA foams (with the same constitutive material), the plot of $\overline{K_{Ic}} = f(\rho^*/\rho_s)$ does not seem sufficient to conclude on an effect of cell size on the fracture properties.

As uncertainties remain on the dissociation of the effect of the constitutive material and the cell size, this raises the question of what parameter is really representative of the fracture toughness of polymeric foams. Geometric parameters like the amount of substantial crack surface as proposed by Jelitto and Schneider (159) could be a key to better understand fracture tests on foams with very different cellular structures as micro and nanocellular foams.

Impact properties of foams

Understanding the behaviour of foams under impact is paramount for applications ranging from packaging materials to automotive components where there are high-speed loading-rate environments (165; 166). That is why, the impact properties of polymeric cellular foams usually refer to their fracture properties under dynamic loadings using energetic characterisation methods. This type of loading can generate a response of the specimen different than in quasi-static due to several phenomena like the visco-elastic response of the constitutive materials (52). This section will focus on these kinds of solicitations. However, it should be noted that a strain-rate dependency can also be associated with the cracking regime. One then speaks of dynamic fracture for materials that can be brittle. For polymeric materials, the fracture energy varies according to the cracking regime. For amorphous thermoplastic and thermosetting polymers, the fracture energy increases with the cracking velocity (120; 118; 117). While for rubber toughened and semi-crystalline thermoplastic polymers, the fracture energy decreases with the cracking velocity (116; 118; 119).

Test methods

The tests described in the previous section on fracture properties, using SENT or SENB specimens, can be performed in dynamic conditions. However, there is much less data available for dynamic displacement speeds (see tab. 3). A study of the fracture properties of mesocellular PVC foams ($\rho^* = 260\ kg\ m^{-3}$) in the dynamic regime yielded a toughness of 2.74 $MPa\ m^{0.5}$, which is 3.75 times higher than the quasi-static toughness (107). In the case of expanded mesocellular polystyrene bead foams (EPS), a compact tension (CT) geometry was used coupled with a falling mass (163). The fracture behaviour of polyurethane foams has more recently been studied in dynamic (164), because of its use as a core in a sandwich structure. Three-point bending tests on a notched specimen were carried out using a pendulum. Fracture toughness is deduced using the same equations as for the static case (141). It has been shown on PU foams that toughness is strongly dependent on the strain rate, with a higher dynamic fracture toughness than the static one (139; 157). From tab. 3, it can be seen that these dynamic fracture tests were carried out mostly on mesocellular polymeric foams.

The majority of the impact tests performed to study the fracture properties of microcellular and nanocellular foams differ from the previously presented fracture tests in that they offer a more basic approach (167). With Charpy, Izod or Gardner impact tests, it is a purely energetic approach with no mechanical model behind the post-processing of the

Article	Base material	Test	Dim. (mm^3)	Impact energy (J)	Cell size	ρ^*/ρ_s (-)
Mesocellular foams						
Mills and Kang, 1994 (163)	EPS	CT	50×50×20	5.5	100 μm	0.02-0.07
Kabir et al., 2006 (107)	PVC	SENB	25×12.5×100	17-45	200 - 500 μm	0.05 - 0.2
Kabir et al., 2006 (107)	PUR	SENB	25×12.5×100	17-45	100 μm	0.2
Marsavina et al, 2013 (164)	PUR	SENB	13×25×100	7.5	50 - 200 μm	0.03 - 0.13
Microcellular foams						
Gomez-Monterde et al., 2016 (64)	ABS	SENT	44×10×5	15	5 - 47 μm	0.83 and 0.90

Table 3. Assessment of the various experimental campaigns carried out on the fracture behaviour of foams in the dynamic regime. x: when no mention of the given parameter was made in the article.

data, which prevents structural effects from being taken into account in the analysis of the fracture properties. The impact strength measured in these tests reflect the combination of different fracture mechanisms (e.g., crack initiation, growth and coalescence), which are not controlled in impact testing. Furthermore, notch geometry and the constitutive material properties can modify the influence of each of these mechanisms.

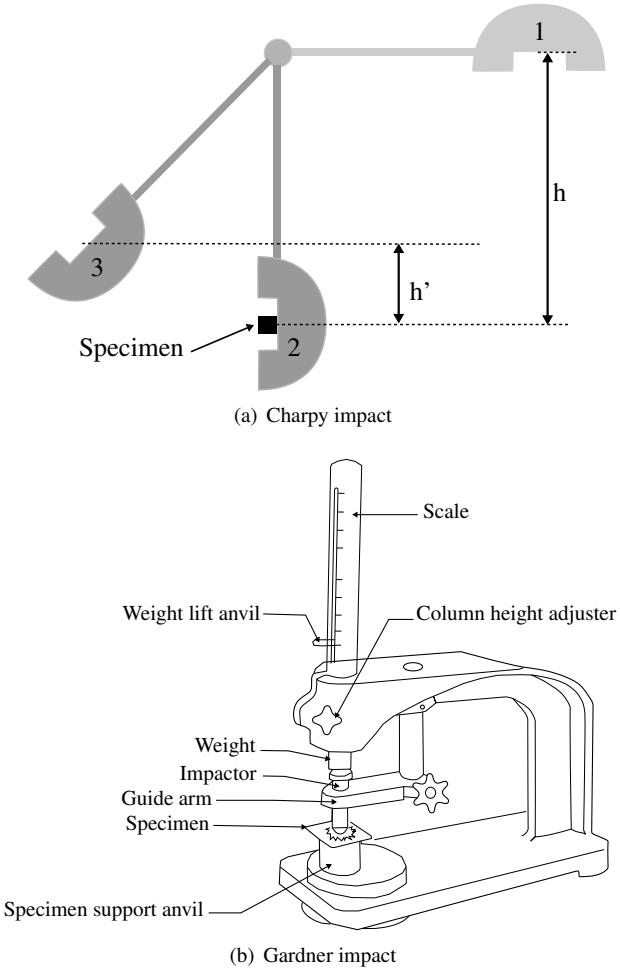

(a) Charpy impact

(b) Gardner impact

Figure 14. Testing devices for impact tests.

Charpy impact The Charpy impact test is a standardised impact test (at high strain-rate) performed to determine the amount of energy absorbed by a material during fracture. The Charpy impact tester is a pendulum device (fig. 14a). The specimen size is defined by norms like the ISO 179-1 (168) and usually stands around 10×10×55 mm^3 in order to be in plane strain conditions. The specimen is notched and the geometry of the notch affects the results of the impact test (as well as the temperature and the strain-rate).

The specimen is fractured as the pendulum swings through, the height of the swing being a measure of the amount of energy absorbed in fracturing the specimen (fig. 14a). In classical calculations, the friction and dynamic effects are neglected.

Gardner impact Falling dart impact, also known as Gardner impact, is a traditional method for evaluating the impact strength or toughness of a polymeric material (169). The test is often used to specify appropriate materials for applications involving impact or to evaluate the effect of secondary finishing operations or other environmental factors on polymers impact properties. A weight is raised inside a guide tube to a predetermined height, then released to drop onto the top of the impactor, forcing the nose through the test sample (fig. 14b). The main result is a pass / fail information. The results from the 20 impacts are used to calculate the Mean Failure Height the point at which 50% of the test samples will fail under the impact.

Izod impact The Izod impact test is another standardised impact test, like with the ASTM D256 standard (170). The principle is roughly the same as for the Charpy test. However several discrepancies can be noticed as instead of a 3-point bending test it is a recessed bending test. The specimen is also notched but presents a larger length (75 mm). One extremity is vertically recessed until near the notch. A horizontal knife instead of a vertical one impacts the notched face of the free end.

Unlike the Charpy impact test (108; 171; 172; 97) and the Gardner impact test (108; 173; 96; 174), the Izod impact test has been much less used to determine the fracture properties under impact of polymeric foams (8; 21), as shown in tab. 4.

Comparison Generally, a material is stressed with only one of the test means and this differs according to the material (tab. 4). The comparison of results obtained with these different test means is delicate. Waldman measured the notched Charpy impact strength of a microcellular PS foam and found it to be higher than that of the pure polymer, whereas in a falling mass experiment, a Gardner impact test, the impact strength was lower than that of the pure polymer matrix (108). Therefore, the study of the influence of the cell size on the obtained material properties cannot be carried out by comparing the results of these different studies and only the results of each study will be presented independently.

Influence of cell size on impact properties

Since 1994, when very few studies could be identified, a relatively large number of microcellular polymeric foams have had their impact behaviour investigated through various characterisation methods (tab. 4). Microcellular foams have attracted considerable attention as their mechanical properties, particularly those related to fracture and impact, have been reported to be similar, if not higher, to those of their unexpanded counterparts (94). Fewer studies have been made on nanocellular foams (like for other material parameters). All of these studies have been realised on a large range of polymers, amorphous for the most part: PP, PS, PC, PVC, PEI, PMMA (see tab. 4).

Notched Charpy and Izod Work done on the impact behaviour of mesocellular foams does not show any particular cell size effect according to Saiz-Arroyo et al.. Tests made on PP foams with relative densities from 0.3 to 0.6 indicated that it was the open-cell content that was a more important parameter to take into account for impact properties (172). A significant increase in Charpy V-notch impact strength of PC microcellular foams was reported for a relative density bellow 0.80 and an average cell size of 40 μm (fig. 15). Lower cell size of 10-20 μm with higher relative densities did not result in such improvements (171). On the other hand, U-notched samples demonstrated a decrease in their Charpy work in comparison to unfoamed PC.

The notched Izod impact strength of PC microcellular foams with a relative density of 0.7 studied by Barlow et al. was multiplied by 2 as the cell size increased from 7 to 18 μm (8). No change in mechanism is observed and all specimens demonstrated a brittle fracture. Although the PC foams studied by Barlow et al. show an improvement in impact resistance compared to their unexpanded version, the increase in impact resistance at higher average cell size, in the range of 18-40 μm, is not consistent with the definition of microcellular foams and is not in agreement with the upper limit of defect size.

Concerning microcellular PS foams, Charpy impact tests showed an increase of the Charpy fracture work with the relative density (108). For all densities, the value was higher than the bulk one (fig. 15). A brittle/ductile transition was furthermore observed when the cell size of the microcellular PS foam was less than 5 μm (108).

For PEI foams, Miller and Kumar also demonstrated with Charpy impact tests that nanocellular foams had better impact strength per unit thickness than microcellular foams (fig. 15). Their value was even more important than unfoamed materials. A brittle to ductile transition in nanocellular foams has also been observed in uniaxial quasi-static tensile tests (96). According to the authors, that is the same mechanism that would lead to a better response to impact tests, with impact energies up to 600 % higher than those of microcellular foams (fig. 15).

The impact behaviour tested by Charpy impact tests on PMMA microcellular and nanocellular foams seem also to show an increase of the impact properties with the cell size decreasing (97). Notario et al. decided to draw the impact resistance divided by the square of the relative density as a function of the size. They also draw the

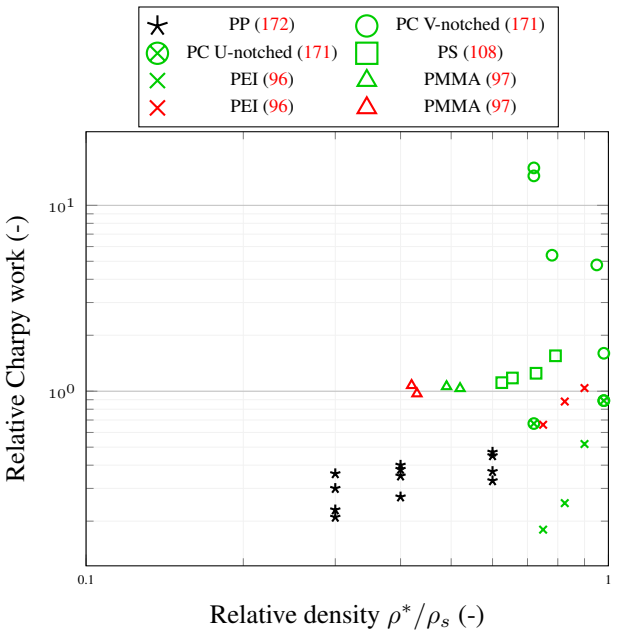

Figure 15. Relative data obtained from Charpy impact as a function of relative density. In black, mesocellular foams. In green, microcellular foams. In red, nanocellular foams (log-log scale).

value of the solid material which they assume around 15 kJ/m^2. However, when these results are analysed through the relative density, no important discrepancies between nanocellular and microcellular can be observed (fig. 15). Both demonstrate an impact behaviour that is similar to unfoamed material but with a smaller relative density. Izod impact tests realised by Wang et al. seems also to conclude on a enhancement of the PMMA impact properties with the introduction of nanoscopic porosities (21).

There are a number of possible reasons for these contradictory results. The choice of a Charpy or Izod test changes the methods of specimen preparation. Different types of notches with a change in the type of notch bottom (damage, micro-cracking, heating or local melting) are then obtained and may explain most of these results. This is particularly true in the presence of cells of different sizes in the vicinity of the notch. These phenomena are even more complex when comparing foams based on different polymers due to their different notch sensitivities. For these reasons, comparison of Charpy or Izod impact response is quite difficult and should be reserved for quality control and material specifications, as stipulated by ASTM.

Gardner impact As for Charpy impact tests, Waldman observed a brittle/ductile transition during Gardner impact tests when the cell size of a PS foam was less than 5 μm (108). The thickness of the skin has been shown to have an influence on the impact resistance given by the Gardner tests. A microcellular foam with a 10 μm thick skin instead of the typical 100 μm demonstrated a 18% higher impact strength. It is because the test relies on bending stress to initiate a crack and therefore the crack initiates at the surface.

Kumar et al. have demonstrate that the crystallinity weight strongly modifies the relative impact strength. Considering crystallized poly(ethylene terephthalate) (CPET) foamed at different pressures, they obtained CPET microcellular foams

Article	Base Material	Test	Dimensions (mm^3)	Speed (m/s)	Cell size	ρ^*/ρ_s (-)
Mesocellular foams						
Saiz et al., 2013 (172)	PP	Charpy	ISO 179-1/1eA	x	50 - 350 μm	0.3-0.6
Microcellular foams						
Waldman, 1982 (108)	PS	Charpy	10.2 × 63.5 × t	x	5-9 μm	0.5 - 1
Waldman, 1982 (108)	PS	Gardner	127 × 76 × t	x	1 - 80 μm	0.5 - 1
Collias et al., 1994 (171)	PC	Charpy	half of ASTM standards	1 - 2.5	10 - 45 μm	0.72 - 0.98
Juntunen et al., 2000 (173)	PVC	Gardner	1×10×10	x	1 - 3 μm	0.6 - 1
Kumar et al., 2000 (175)	CPET	Gardner	50×50×t	x	x	0.5 - 1
Barlow et al., 2001 (8)	PC	Izod	ASTM D256	x	4 - 18 μm	0.33-0.9
Miller et al., 2011 (96)	PEI	Gardner	2×50×50	x	2 - 5 μm	0.75-0.9
Notario et al., 2015 (97)	PMMA	Charpy	ISO 179-1	0.5	7-11 μm	0.49-0.52
Nanocellular foams						
Miller et al., 2011 (96)	PEI	Gardner	2×50×50	x	20 - 130 nm	0.75-0.9
Notario et al., 2015 (97)	PMMA	Charpy	ISO 179-1	0.5	200-360 nm	0.4
Wang et al., 2017 (21)	PMMA/TPU	Izod	ASTM D256	x	1.3 - 0.5 μm	0.23-0.32

Table 4. Assessment of the various experimental campaigns carried out on the mechanical behaviour of nanocellular foams under impact. x: when no mention of the given parameter was made in the article.

with different crystallinity weights. The foams obtained at lower pressures (3 and 4 MPa) had a similar crystallinity weight to that of the dense CPET (10.4%) and are referred to as CPET LC for Low Crystallinity in fig. 16. These foams demonstrate a low impact strength. A pressure of 5 MPa gave however a CPET microcellular foam with a crystallinity weight of 38.5% (referred to as HC for High Crystallinity). The Gardner impact response of these foams were almost similar to that of the dense CPET. The dense CPET tested has however a crystallinity weight of 10.4%, direct comparison is therefore complex.

Microcellular PVC foams showed an increasing impact resistance with its relative density (173). An opposite effect was observed by Miller et al. on microcellular PEI foams. The impact strength per unit thickness of PEI microcellular foams decreased with increasing relative density (96). But the impact strength per unit thickness of nanocellular PEI foams increased with the relative density. The densest nanocellular PEI foams even showed higher values than bulk PEI (96).

Further analysis The mechanical properties measured either by Charpy, Izod or Gardner impact on different polymeric foams (PC, PS, PEI, PMMA, CPET) mainly seem to show the same trend (fig. 15 and fig. 16). The introduction of very small porosities (below 100 μm) seems to greatly enhance the impact toughness of polymers. Several times, a fragile to ductile transition was observed at the sample surface (108; 96). This effect has been attributed to an inherently critical defect size, below which the cells do not behave as defects but allow the release of tri-axial stresses. However, it appears other parameters as the crystallinity weight need to be taken into account for semi-crystalline microcellular foams to fully isolate the cell size effect (175).

Brief summary of the impact properties

With regard to the influence of cell size on the fracture properties, it would appear that current knowledge shows that in quasi-static and dynamic conditions, a reduction in cell size is beneficial.

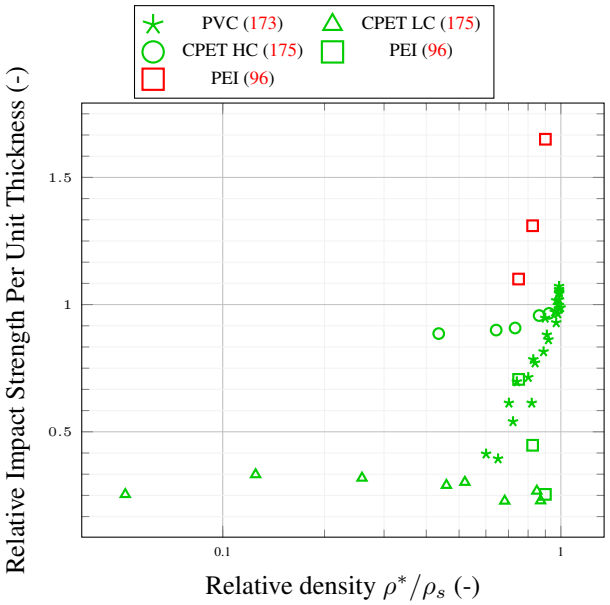

Figure 16. Relative data obtained from Gardner impact as a function of relative density. In green, microcellular foams. In red, nanocellular foams (linear-log scale).

As far as impact behaviour is concerned, Charpy impact and Gardner impact are the most commonly used methods. These types of tests are purely energetic impact test. It prevents to obtain a material parameter, independent of the specimen geometry. Therefore, no direct comparison can be made between the different studies using either Charpy impact tests or Gardner impact tests. The accessibility of these tests is however useful for many researchers and if one had to choose, the Charpy test seems preferable to the Gardner test. Many results concerning microcellular and nanocellular polymeric foams seem to show that the decrease in cell size has a significant effect on improving the impact properties of the polymers. The impact properties of these microcellular and nanocellular polymeric foams are similar or even better than those of their dense base material. More

results on nanocellular polymeric foams with similar test methods would allow to confirm this trend.

Discussion

Current results on nanocellular polymeric foams seem to show that reducing the cell size mainly improves the non-linear mechanical behaviour of the foams (fracture and impact properties). The potential sources of the change in mechanical behaviour due to a size effect can have two different origins. On one hand, nanocellular foams display much thinner cell walls than microcellular foams (34; 15; 176). This important decrease in the cell wall thickness can lead to a change in the organisation of macromolecules in the cell wall known as a "thin-film effect". This leads to a change in the mechanical behaviour of the base material and can be considered a material effect at the nanoscale. On the other hand, there may be a cell size small enough that the cell is no longer considered as a defect by the whole structure. This effect can be considered as a structural effect at the nanoscale. Both of these potential sources are discussed in the following subsections.

Thin film effect

Below a certain thickness, some researchers think that cell walls in foams are so thin they may be equivalent to thin films (101; 179). This means that the chains of the constitutive polymer material are confined within the cell walls of the nanocellular foams. It was shown with diffuse neutron scattering experiments that the minimum thickness for such confinement to occur in polymer films is of the order of six times the radius of gyration r of the polymer chains (180). Previous works on PMMA demonstrated that conformational changes and immobilization of the PMMA chains could also be observed for PMMA nanoporous polymers thanks to Raman and dielectric spectroscopy (178). In the case of PMMA, which is the most studied nanocellular foam, the radius of gyration is about 7.97 nm for an average molecular weight M_w= 83,000 g/mol as the one studied by Pinto et al. (178). It is defined by the eq. 19 (181),

$$< r^2 >= 0.096 \cdot M_w^{0.98}. \quad (19)$$

Therefore, a confinement effect should be observed for this type of PMMA when cell walls are about 47 nm or below.

Studies on dense polymeric thin films have demonstrated that this confinement can cause a modification of the glass transition temperature (T_g) in comparison to bulk polymers (182; 183; 184). It appears that thin films demonstrate a lower glass transition temperature than bulk (185; 186). Free-standing thin polymer films especially display large reduction in their T_g. However this reduction is not related to the enhancement of entire chain motion (186). The apparent modulus of PMMA ultra-thin films (from 200 nm to 5 nm) is comparable to the bulk above a thickness of 40 nm. Below 40 nm, issues in mechanical stability and robustness make the modulus drops drastically (187).

To verify if a confinement of the macromolecular chains takes place within the cell walls of the nanocellular foams, the T_g of these foams was thus generally studied. Several studies have measured the modification of the glass transition temperature between micro or nanocellular PMMA, PMMA-MAM and PEI foams and their constitutive material either by DSC (Differential Scanning Calorimetry) or by 3-point bending DMA (tab. 5). DMA tests were carried out on a larger number of specimen varieties (PMMA and PMMA-MAM at different frequencies) (101). The authors showed that below a cell wall thickness of 100 nm, the T_g increased significantly. It could increase from 115°C for the dense material to 126°C for the foam with the thinnest cell walls. Notario et al. also noted a 7°C increase in glass transition temperature using DMA tests for nanocellular PMMA foams (97). Furthermore, the influence of pressure and saturation temperature on the glass transition temperature was studied by Pinto (101). The results showed an absence of influence of processing parameters on the T_g for PMMA foams. In the case of PEI foams, an increase in the T_g of the polymer matrix was observed (96).

A noticeable increase in the glass transition temperature was thus observed for nanocellular PMMA (33; 97; 177), PMMA-MAM (33) and PEI (96) foams (tab. 5). The deviation from the bulk material glass transition temperature is visible as function of the relative density in fig. 17. It should be noted that all the foams studied have a fairly high relative density (>0.24). It appears that the variation of the deviation does not vary across the small range of relative densities for PMMA and PEI microcellular foam. This deviation is most of the time close to 0. On the contrary, the deviation of the glass transition temperature of PMMA and PEI nanocellular foams seems to really depend on the relative density of the foam. The lighter the nanocellular foam, the more important the deviation. At the smallest relative density (0.24), the deviation for nanocellular PMMA foams reaches 12°C.

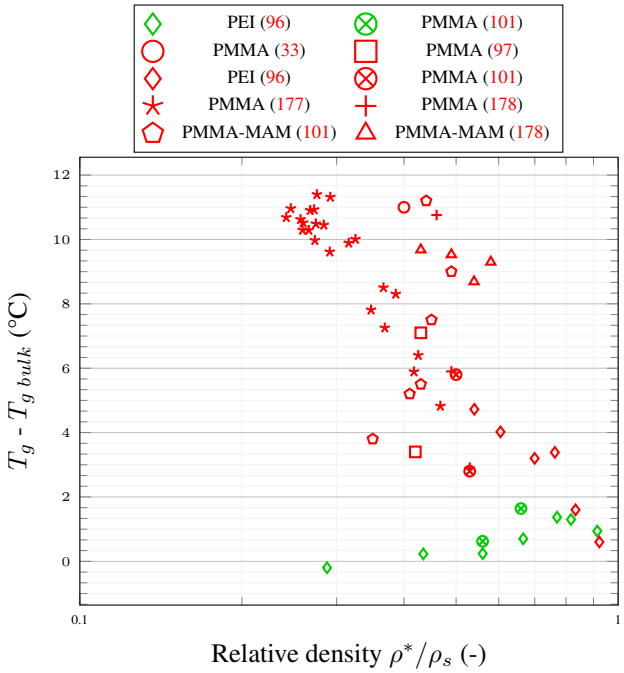

Figure 17. Difference between the glass transition temperature of the constitutive material $T_{g\ bulk}$ and the glass transition temperature of the cellular material T_g. In black, mesocellular foams. In green, microcellular foams. In red, nanocellular foams (linear-log scale).

Article	Base material	Test	T_g bulk °C	T_g micro °C	T_g nano °C	Cell size nm	ρ^*/ρ_s -
Reglero-Ruiz et al. 2011 (33)	PMMA/MAM	DMA	112	x	123	200-300	0.4
Miller et al. 2011 (96)	PEI	DSC	216.4	216 - 218	217 - 221	20 - 5000	0.3-0.9
Pinto, 2014 (101)	PMMA-MAM	DSC	122.6	121.4 - 124.8	126.1 - 129.7	150-1870	0.36-0.58
Notario et al., 2015 (97)	PMMA	DMA	122.6	121.4 - 124.8	126.1 - 129.7	200-600	0.42
Martin-de-Leon, 2016 (177)	PMMA	DSC	114.5	x	119.5-125	20-84	0.24-0.53
Pinto et al., 2017 (178)	PMMA	DSC	112	112.6 - 113.6	115 - 123	90 - 200	0.46 - 0.49
Pinto et al., 2017 (178)	PMMA-MAM	DSC		x	x	150 - 190	0.43 - 0.58

Table 5. Summary of the different experimental campaigns carried out on the glass transition temperature of nanocellular foams. x: when no mention of the given parameter was made in the article.

For the PEI foams, Miller and Kumar observed that as the relative density is decreasing, the cell wall thickness reduces from 300 nm (ρ_r = 0.7) to within the range of 100-200 nm (ρ_r = 0.6-0.47) and the T_g increases by 5°C (96). The PMMA nanocellular foams studied by Martin-de-Leon displayed a constant cell wall thickness (177). However, it was noticed that the volume fraction of the solid contained in the edges of the cell ϕ was linearly linked to the relative density. So although cell wall thickness remains constant, cell edges thickness reduce with relative density reduction.

Polymeric nanocellular foams present therefore a higher glass transition temperature than microcellular polymeric foams. Several authors concluded that it was the sign that a change in cell size scale from micro to nano does have a local influence on the macromolecular chains arrangement in the cell walls (33; 96; 97; 177). However, there are a number of arguments against this conclusion. (1) These glass transition temperature values are still in agreement with the T_g values of the PMMA chains (between 100 and 130°C) and PEI (around 217°C) which depend mainly on the molar mass, the co-monomer content, the chain entanglement, the tacticity and, secondarily, the surface effects. (2) A partial chain elongation in the course of foaming could also be the source of this enhancement (33). (3) Finally, as explained above, for free-standing thin films, a decrease of the glass transition temperature is usually observed (186), unlike what is observed in the studies detailed in tab. 5 and fig.17.

It appears the enhancement of the glass transition temperature in nanocellular foams is still a subject to clarify. Perhaps traditional techniques used until now (DMA, DSC) do not have sufficient sensitivity. It might be interesting to use techniques similar to the ones used for thin films to probe the glass transition and entire chain motion (184; 186; 188). It would allow to experimentally confirm that locally, nanocellular foams are different to meso and microcellular foams explaining the change in the mechanical behaviour.

Plane-strain to plane-stress

The fact that only the non-linear mechanical behaviour of foams seems to be affected by the cell size reduction do not point to a nanoscale effect at the cell wall scale. Several researchers have also formulated the hypothesis that below a specific size, a cell is not considered as a defect by the structure anymore.

Small porosities would act the same way rubber particles in polymers like ABS (171). By internal cavitation, they may relieve the triaxial stress state in front of the crack tip (189). This mechanism would only happen if the cell size is small enough to transform plane-strain (strain vector is zero across a particular plane) into plane-stress conditions (stress vector is zero across a particular plane). Plane-strain fracture toughness is generally lower than plane stress in standard continuum solids. This would be the reason explaining the brittle to ductile fracture transition and thus tougher fracture observed in many cases (108; 96).

Recent research on the fracture toughness of metamaterials demonstrated that unlike conventional dense materials, the plane-stress toughness of lattices metamaterials is lower than the plane-strain toughness (190). While previous studies on this type of materials only focused on K_{I_c} (191; 192; 193; 194), they demonstrated with experimental and numerical work that in addition to K_{I_c}, T-stresses need to be taken into account to analyse the fracture toughness of those heterogeneous materials.

Conclusion and Perspectives

The race for nanocellular foams is driven in part by the lure of physical properties, including mechanical properties, beyond the conventional mechanical framework. The transition to the nanoscale is announced as a great leap towards new materials. Several works concerning the mechanical behaviour of microcellular and nanocellular polymeric foams have been realised. The main goal of these studies is generally to produce foams with the smallest cell size and the smallest density. They do not focus their discussion on their mechanical results. That is why this review has been undertaken.

The compilation of these research works shows that as far as the linear mechanical properties in compression are concerned, this leap does not seem to be as great as announced. In the density ranges tested, the relative Young's modulus and the relative buckling stress of microcellular and nanocellular foams stay mainly function of the relative density of the foam.

On the other hand, the impact properties studied by Charpy, Izod and Gardner impact tests are clearly enhanced by the introduction in the polymer of small porosities (below 100 μm for most polymers, *i.e.* micro and nanocellular foams). The reason of the increase of the impact toughness would be close to the effect of rubber particles inside polymeric matrix. Small porosities seem to relieve the triaxial stress state at the tip of the crack resulting in a ductile and thus tougher material.

The results on the fracture properties obtained by non-dynamic means are less compelling. An effect of the cell size

reduction seems to happen. However a similar methodology for all should be put in place in order to be able to confirm this hypothesis based on a specific data representation.

More generally, in order to confirm or refute these conclusions, it seems necessary to increase the number of data concerning the mechanical behaviour of nanocellular polymer foams. The buckling stress and the fracture toughness remain little studied for these types of foams. It is necessary to set up common methodologies between the different research teams working on this subject, especially concerning the non-linear mechanical properties where many different ones have been used over the years. Furthermore, research work has mainly been focused on the quasi-static properties (aside from impact) at room temperature. In order to enrich the conclusion on a size effect on the mechanical behaviour of foams, it is necessary to study these foams over a wider range of strain rates and temperature. Carrying out mode I fracture tests on notched geometries seems to be the right way to go, making sure to scan sufficiently wide cracking regimes (from quasi-static to dynamic). This will probably make it possible to dissociate the effects of the constitutive materials from those of the cell size. Finally theories behind a specific nanoscale effect on the mechanical behaviour of polymeric foams need to be confirmed. Closer observations of the cell walls could allow to confirm the hypothesis of a confinement of the molecular chains.

CRediT authorship contribution statement

Louise Le Barbenchon: Conceptualization, Investigation, Visualization, Writing – original draft, Writing – review and editing. **Jean-Benoît Kopp**: Writing – original draft.

Acknowledgements

This research was supported by the french ANR edyFiCE project under the grant number ANR-18-CE06-0030. The authors thank Michel Dumon (LCPO) for coordinating this project.

Data Availability

The raw/processed data required to reproduce these findings cannot be shared at this time due to technical or time limitations. It is however available on request.

References

[1] Fleck NA, Deshpande VS and Ashby MF. Micro-architectured materials: Past, present and future. *Proceedings of the Royal Society A: Mathematical, Physical and Engineering Sciences* 2010; 466(2121): 2495–2516. DOI: 10.1098/rspa.2010.0215.

[2] Baekeland LH. Method of making insoluble products of phenol and formaldehyde. *United States Patent Office* 1909; : 3.

[3] Obi BE. Applications of Polymeric Foams in Automobiles and Transportation. *Polymeric Foams Structure-Property-Performance* 2018; : 341–366DOI: 10.1016/b978-1-4557-7755-6.00012-4.

[4] Verdejo R and Mills N. Performance of EVA foam in running shoes. In *The Engineering of Sport*, volume 4. Kyoto, Japan: Blackwell Science. ISBN 978-0-632-06481-6, 2002. pp. 580–588.

[5] Mills NJ and Masso-Moreu Y. Finite Element Analysis (FEA) applied to polyethylene foam cushions in package drop tests. *Packaging Technology and Science* 2005; 18(1): 29–38. DOI:10.1002/pts.676.

[6] Gibson LJ and Ashby MF. *Cellular Solids: Structure and Properties*. Oxford: Cambridge University Press, 1997.

[7] Kumar V. Microcellular polymers: Novel materials for the 21st century. *Progress in Rubber & Plastics* 1993; 9(1): 54–70.

[8] Barlow C, Kumar V, Flinn B et al. Impact strength of high density solid-state microcellular polycarbonate foams. *Journal of Engineering Materials and Technology, Transactions of the ASME* 2001; 123(2): 229–233. DOI: 10.1115/1.1339004.

[9] Kumar V, VanderWel M, Weller J et al. Experimental characterization of the tensile behavior of microcellular polycarbonate foams. *Journal of Engineering Materials and Technology, Transactions of the ASME* 1994; 116(4): 439–445. DOI:10.1115/1.2904310.

[10] Wing G, Pasricha A, Tuttle M et al. Time dependent response of polycarbonate and microcellular polycarbonate. *Polymer Engineering and Science* 1995; 35(8): 673–679. DOI:10.1002/pen.760350807.

[11] Handa YP and Zhang Z. A New Technique for Measuring Retrograde Vitrification in Polymer – Gas Systems and for Making Ultramicrocellular. *Journal of Polymer Science Part B: Polymer Physics* 2000; 38: 716–725.

[12] Yokoyama H and Sugiyama K. Nanocellular structures in block copolymers with CO_2-philic blocks using CO_2 as a blowing agent. *Polymer Preprints, Japan* 2006; 55(1): 936.

[13] Sharudin RWB and Ohshima M. CO_2-induced mechanical reinforcement of polyolefin-based nanocellular foams. *Macromolecular Materials and Engineering* 2011; 296(11): 1046–1054. DOI:10.1002/mame.201100085.

[14] Costeux S. CO_2-blown nanocellular foams. *Journal of Applied Polymer Science* 2014; 131(23). DOI:10.1002/app.41293.

[15] Pinto J, Dumon M, Pedros M et al. Nanocellular CO_2 foaming of PMMA assisted by block copolymer nanostructuration. *Chemical Engineering Journal* 2014; 243: 428–435. DOI:10.1016/j.cej.2014.01.021.

[16] Bernardo V, Van Loock F, Martin-de Leon J et al. Mechanical Properties of PMMA-Sepiolite Nanocellular Materials with a Bimodal Cellular Structure. *Macromolecular Materials and Engineering* 2019; 304(7): 1–12. DOI:10.1002/mame.201900041.

[17] Yeh SK, Demewoz NM and Kurniawan V. Controlling the structure and density of PMMA bimodal nanocellular foam by blending different molecular weights. *Polymer Testing* 2021; 93: 107004. DOI:10.1016/j.polymertesting.2020.107004.

[18] Haurat M, Tassaing T and Dumon M. FTIR in situ measurement of swelling and CO_2 sorption in acrylic polymers at high CO_2 pressures. *Journal of Supercritical Fluids* 2022; 182(September 2021): 105534. DOI:10.1016/j.supflu.2022.105534.

[19] Martin-de Leon J, Van Loock F, Bernardo V et al. The influence of cell size on the mechanical properties of

nanocellular PMMA. *Polymer* 2019; 181(September): 121805. DOI:10.1016/j.polymer.2019.121805.

[20] Notario B, Pinto J, Solorzano E et al. Experimental validation of the Knudsen effect in nanocellular polymeric foams. *Polymer* 2015; 56: 57–67. DOI:10.1016/j.polymer.2014.10.006.

[21] Wang G, Zhao J, Mark LH et al. Ultra-tough and super thermal-insulation nanocellular PMMA/TPU. *Chemical Engineering Journal* 2017; 325: 632–646. DOI:10.1016/j.cej.2017.05.116.

[22] Martini-Vvedensky JE, Suh NP, Church F et al. Microcellular Closed Cell Foamsand Their Method of Manufacture. *United States Patent Office* 1984; .

[23] Colton JS. A method of producing microcellular foams and microcellular foams of semi-crystalline polymeric materials. *United States Patent Office* 1989; .

[24] Kumar V and Suh NP. A process for making microcellular thermoplastic parts. *Polymer Engineering & Science* 1990; 30(20): 1323–1329. DOI:10.1002/pen.760302010.

[25] Park CB, Suh NP and Baldwin DF. Method for Providing Continuous Processing of Microcellularand Supermicrocellular Foamed Materials. *United States Patent Office* 1999; .

[26] Dong Hwang Y and Woon Cha S. The relationship between gas absorption and the glass transition temperature in a batch microcellular foaming process. *Polymer Testing* 2002; 21(3): 269–275. DOI:10.1016/S0142-9418(01)00081-2.

[27] Dong G, Zhao G, Guan Y et al. The cell forming process of microcellular injection-molded parts. *Journal of Applied Polymer Science* 2014; 131(12): 1–11. DOI:10.1002/app.40365.

[28] Di Maio E and Kiran E. Foaming of polymers with supercritical fluids and perspectives on the current knowledge gaps and challenges. *The Journal of Supercritical Fluids* 2018; 134: 157–166. DOI:10.1016/j.supflu.2017.11.013.

[29] Notario B, Pinto J and Rodriguez-Perez MA. Nanoporous polymeric materials: A new class of materials with enhanced properties. *Progress in Materials Science* 2016; 78–79: 93–139. DOI:10.1016/j.pmatsci.2016.02.002.

[30] Martín-de León J, Bernardo V and Rodríguez-Pérez MÁ. Nanocellular polymers: The challenge of creating cells in the nanoscale. *Materials* 2019; 12(5): 1–19. DOI:10.3390/MA12050797.

[31] Ruiz JAR, Marc-Tallon J, Pedros M et al. Two-step micro cellular foaming of amorphous polymers in supercritical CO_2. *Journal of Supercritical Fluids* 2011; 57(1): 87–94. DOI:10.1016/j.supflu.2011.01.011.

[32] Martin-de Leon J, Bernardo V and Rodriguez-Perez MA. Low density nanocellular polymers based on PMMA produced by gas dissolution foaming: Fabrication and cellular structure characterization. *Polymers* 2016; 8(7). DOI:10.3390/polym8070265.

[33] Reglero Ruiz JA, Dumon M, Pinto J et al. Low-density nanocellular foams produced by high-pressure carbon dioxide. *Macromolecular Materials and Engineering* 2011; 296(8): 752–759. DOI:10.1002/mame.201000346.

[34] Ruiz JAR, Pedros M, Tallon JM et al. Micro and nano cellular amorphous polymers (PMMA, PS) in supercritical CO_2 assisted by nanostructured CO_2-philic block copolymers - One step foaming process. *Journal of Supercritical Fluids* 2011; 58(1): 168–176. DOI:10.1016/j.supflu.2011.04.022.

[35] Pinto J, Pardo S, Solorzano E et al. Solid skin characterization of PMMA/MAM foams fabricated by gas dissolution foaming over a range of pressures. *Defect and Diffusion Forum* 2012; 326–328: 434–439. DOI:10.4028/www.scientific.net/DDF.326-328.434.

[36] Bernardo V, Martin-de Leon J, Laguna-Gutierrez E et al. Understanding the role of MAM molecular weight in the production of PMMA/MAM nanocellular polymers. *Polymer* 2018; 153(July): 262–270. DOI:10.1016/j.polymer.2018.08.022.

[37] Bernardo V, Martin-de Leon J, Pinto J et al. Low-density PMMA/MAM nanocellular polymers using low MAM contents: Production and characterization. *Polymer* 2019; 163(August 2018): 115–124. DOI:10.1016/j.polymer.2018.12.057.

[38] Haurat M and Dumon M. Amorphous Polymers' Foaming and Blends with Organic Foaming-Aid Structured Additives in Supercritical CO_2, a Way to Fabricate Porous Polymers from Macro to Nano Porosities in Batch or Continuous Processes. *Molecules* 2020; 25(22). DOI:10.3390/molecules25225320.

[39] Guo H, Nicolae A and Kumar V. Solid-state poly(methyl methacrylate) (PMMA) nanofoams. Part II: Low-temperature solid-state process space using CO_2 and the resulting morphologies. *Polymer* 2015; 70: 231–241. DOI:10.1016/j.polymer.2015.06.031.

[40] Forest C, Chaumont P, Cassagnau P et al. Nanofoaming of PMMA using a batch CO_2 process: Influence of the PMMA viscoelastic behaviour. *Polymer* 2015; 77: 1–9. DOI:10.1016/j.polymer.2015.09.011.

[41] Martin-de Leon J, Bernardo V and Rodriguez-Perez MA. Key Production Parameters to Obtain Transparent Nanocellular PMMA. *Macromolecular Materials and Engineering* 2017; 302(12): 3–7. DOI:10.1002/mame.201700343.

[42] Costeux S and Zhu L. Low density thermoplastic nanofoams nucleated by nanoparticles. *Polymer* 2013; 54(11): 2785–2795. DOI:10.1016/j.polymer.2013.03.052.

[43] Pinto J, Reglero-Ruiz JA, Dumon M et al. Temperature influence and CO_2 transport in foaming processes of poly(methyl methacrylate)-block copolymer nanocellular and microcellular foams. *Journal of Supercritical Fluids* 2014; 94: 198–205. DOI:10.1016/j.supflu.2014.07.021.

[44] Saiz-Arroyo C, Rodríguez-Pérez MÁ, Velasco JI et al. Influence of foaming process on the structure–properties relationship of foamed LDPE/silica nanocomposites. *Composites Part B: Engineering* 2013; 48: 40–50. DOI:10.1016/j.compositesb.2012.10.045.

[45] Azdast T and Hasanzadeh R. Increasing cell density/decreasing cell size to produce microcellular and nanocellular thermoplastic foams: A review. *Journal of Cellular Plastics* 2021; 57(5): 769–797. DOI:10.1177/0021955X20959301.

[46] Kumar A, Patham B, Mohanty S et al. Polyolefinic nanocomposite foams: Review of microstructure-property relationships, applications, and processing considerations.

Journal of Cellular Plastics 2022; 58(1): 59–102. DOI: 10.1177/0021955X20979752.

[47] Wang X, Mi J, Zhou H et al. Transition from microcellular to nanocellular chain extended poly(lactic acid)/hydroxyl-functionalized graphene foams by supercritical CO_2. *Journal of Materials Science* 2019; 54(5): 3863–3877. DOI: 10.1007/s10853-018-3120-8.

[48] Ni J, Yu K, Zhou H et al. Morphological evolution of PLA foam from microcellular to nanocellular induced by cold crystallization assisted by supercritical CO_2. *Journal of Supercritical Fluids* 2020; 158: 104719. DOI:10.1016/j.supflu.2019.104719.

[49] Sauceau M, Fages J, Common A et al. New challenges in polymer foaming: A review of extrusion processes assisted by supercritical carbon dioxide. *Progress in Polymer Science* 2011; 36(6): 749–766. DOI:10.1016/j.progpolymsci.2010.12.004.

[50] Haurat M, Sauceau M, Baillon F et al. Supercritical CO_2-assisted Extrusion Foaming: A Suitable Process to Produce Very Lightweight Acrylic Polymer Micro Foams. *Journal of Applied Polymer Science* 2022; .

[51] Fratzl P and Weinkamer R. Nature's hierarchical materials. *Progress in Materials Science* 2007; 52(8): 1263–1334. DOI:10.1016/j.pmatsci.2007.06.001.

[52] Sun Y and Li QM. Dynamic compressive behaviour of cellular materials: A review of phenomenon, mechanism and modelling. *International Journal of Impact Engineering* 2018; 112(February 2017): 74–115. DOI:10.1016/j.ijimpeng.2017.10.006.

[53] Meza LR, Zelhofer AJ, Clarke N et al. Resilient 3D hierarchical architected metamaterials. *Proceedings of the National Academy of Sciences of the United States of America* 2015; 112(37): 11502–11507. DOI:10.1073/pnas.1509120112.

[54] Greer JR and Deshpande VS. Three-dimensional architected materials and structures: Design, fabrication, and mechanical behavior. *MRS Bulletin* 2019; 44(10): 750–757. DOI: 10.1557/mrs.2019.232.

[55] Pham MS, Liu C, Todd I et al. Damage-tolerant architected materials inspired by crystal microstructure. *Nature* 2019; 565(7739): 305–311. DOI:10.1038/s41586-018-0850-3.

[56] Jiang H, Le Barbenchon L, Bednarcyk BA et al. Bioinspired multilayered cellular composites with enhanced energy absorption and shape recovery. *Additive Manufacturing* 2020; 36(April): 101430. DOI:10.1016/j.addma.2020.101430.

[57] Dillard T. *Caractérisation et Simulation Numérique Du Comportement Mécanique Des Mousses de Nickel : Morphologie Tridimensionnelle, Réponse Élastoplastique et Rupture*. PhD Thesis, Ecole Nationale Supérieure des Mines de Paris, 2004.

[58] Bouix R, Viot P and Lataillade JL. Polypropylene foam behaviour under dynamic loadings: Strain rate, density and microstructure effects. *International Journal of Impact Engineering* 2009; 36(2): 329–342. DOI:10.1016/j.ijimpeng.2007.11.007.

[59] Chauvet M, Sauceau M, Baillon F et al. Mastering the structure of PLA foams made with extrusion assisted by supercritical CO_2. *Journal of Applied Polymer Science* 2017; 134(28): 45067. DOI:10.1002/app.45067.

[60] Pang Y, Cao Y, Zheng W et al. A comprehensive review of cell structure variation and general rules for polymer microcellular foams. *Chemical Engineering Journal* 2022; 430(P2): 132662. DOI:10.1016/j.cej.2021.132662.

[61] Li J, Chen Z, Wang X et al. Cell morphology and mechanical properties of microcellular mucell ®injection molded polyetherimide and polyetherimide/fillers composite foams. *Journal of Applied Polymer Science* 2013; 130(6): 4171–4181. DOI:10.1002/app.39698.

[62] Chu RKM, Mark LH and Park CB. Scalable Fabrication of Microcellular Open-Cell Polymer Foams. *Advanced Engineering Materials* 2022; 24(3): 2100985. DOI:10.1002/adem.202100985.

[63] Dong G, Zhao G, Guan Y et al. Formation mechanism and structural characteristics of unfoamed skin layer in microcellular injection-molded parts. *Journal of Cellular Plastics* 2016; 52(4): 419–439. DOI:10.1177/0021955X15577149.

[64] Gõmez-Monterde J, Schulte M, Ilijevic S et al. Effect of microcellular foaming on the fracture behavior of ABS polymer. *Journal of Applied Polymer Science* 2016; 133(7): 1–10. DOI:10.1002/app.43010.

[65] Demewoz NM and Yeh SK. Fabrication and characterization of low-density nanocellular foam based on PMMA/TPU blends. *Polymer* 2022; 240(September 2021): 124493. DOI: 10.1016/j.polymer.2021.124493.

[66] Yeh SK, Liao ZE, Wang KC et al. Effect of molecular weight to the structure of nanocellular foams: Phase separation approach. *Polymer* 2020; 191(January): 122275. DOI: 10.1016/j.polymer.2020.122275.

[67] Villanova J, Kumar R, Daudin R et al. Fast In Situ Nanotomography at ESRF. *Microscopy and Microanalysis* 2018; 24(S2): 450–451. DOI:10.1017/S1431927618014496.

[68] Martens I, Vanpeene V, Vostrov N et al. Imaging Voids and Defects Inside Li-Ion Cathode LiNi0.6Mn0.2Co0.2O2 Single Crystals. *ACS Applied Materials & Interfaces* 2023; 15(51): 59319–59328. DOI:10.1021/acsami.3c10509.

[69] Maire E, Elmoutaouakkil A, Fazekas A et al. In situ X-ray tomography measurements of deformation in cellular solids. *MRS Bulletin* 2003; 28(4): 284–289. DOI:10.1557/mrs2003.82.

[70] Maire E. X-Ray Tomography Applied to the Characterization of Highly Porous Materials. *Annual Review of Materials Research* 2012; 42(1): 163–178. DOI:10.1146/annurev-matsci-070511-155106.

[71] Le Barbenchon L, Girardot J, Kopp JB et al. Multi-scale foam : 3D Structure/Compressive Behaviour Relationship Of Agglomerated Cork. *Materialia* 2019; 5(January): 100219. DOI:10.1016/j.mtla.2019.100219.

[72] Barroso-Solares S, Bernardo V, Cuadra-rodriguez D et al. Nanostructure of PMMA/MAM blends prepared by out-of-equilibrium (Extrusion) and near-equilibrium (casting) self-assembly and their nanocellular or microcellular structure obtained from CO_2 foaming. *Nanomaterials* 2021; 11(11). DOI:10.3390/nano11112834.

[73] Cuadra-Rodríguez D, Barroso-Solares S, Rodríguez-Pérez MA et al. Production of cellular polymers without solid outer skins by gas dissolution foaming: A long-sought step towards new applications. *Materials & Design* 2022; 217: 110648. DOI:10.1016/j.matdes.2022.110648.

[74] Gibson LJ. Modelling the mechanical behavior of cellular materials. *Materials Science and Engineering A* 1989; 110(C): 1–36. DOI:10.1016/0921-5093(89)90154-8.

[75] Daphalapurkar NP, Hanan JC, Phelps NB et al. Tomography and simulation of microstructure evolution of a closed-cell polymer foam in compression. *Mechanics of Advanced Materials and Structures* 2008; 15(8): 594–611. DOI:10.1080/15376490802470523.

[76] Bastawros AF, Bart-Smith H and Evans AG. Experimental analysis of deformation mechanisms in a closed-cell aluminum alloy foam. *Journal of the Mechanics and Physics of Solids* 2000; 48(2): 301–322. DOI:10.1016/S0022-5096(99)00035-6.

[77] Kidd TH, Zhuang S and Ravichandran G. In situ mechanical characterization during deformation of PVC polymeric foams using ultrasonics and digital image correlation. *Mechanics of Materials* 2012; 55: 82–88. DOI:10.1016/j.mechmat.2012.08.001.

[78] Maiti SK, Gibson LJ and Ashby MF. Deformation and energy absorption diagrams for cellular solids. *Acta Metallurgica* 1984; 32(11): 1963–1975. DOI:10.1016/0001-6160(84)90177-9.

[79] Dillard T, N'Guyen F, Maire E et al. 3D quantitative image analysis of open-cell nickel foams under tension and compression loading using X-ray microtomography. *Philosophical Magazine* 2005; 85(19): 2147–2175. DOI:10.1080/14786430412331331916.

[80] Kader MA, Islam MA, Saadatfar M et al. Macro and micro collapse mechanisms of closed-cell aluminium foams during quasi-static compression. *Materials and Design* 2017; 118: 11–21. DOI:10.1016/j.matdes.2017.01.011.

[81] Mills NJ. Micromechanics of open-cell foams. In *Polymer Foams Handbook*. Ltd, Butterworth-Heinemann, 2007. pp. 148–175.

[82] Mills NJN. Micromechanics of closed-cell foams. In *Polymer Foams Handbook*. Ltd, Butterworth-Heinemann, 2007. pp. 252–279. DOI:10.1016/b978-075068069-1/50012-x.

[83] Hössinger-Kalteis A, Reiter M, Jerabek M et al. Overview and comparison of modelling methods for foams. *Journal of Cellular Plastics* 2021; 57(6): 951–1001. DOI:10.1177/0021955X20966329.

[84] Jo C, Fu J and Naguib HE. Constitutive Modeling for Characterizing the Compressive Behavior of PMMA Open-Cell Foams. *Journal of Polymer Science Part B: Polymer Physics* 2006; 45: 436–443.

[85] Deshpande VS, Ashby MF and Fleck NA. Foam topology: Bending versus stretching dominated architectures. *Acta Materialia* 2001; DOI:10.1016/S1359-6454(00)00379-7.

[86] Deshpande VS and Fleck NA. Collapse of truss core sandwich beams in 3-point bending. *International Journal of Solids and Structures* 2001; 38(36-37): 6275–6305. DOI:10.1016/S0020-7683(01)00103-2.

[87] Elliott JA, Windle AH, Hobdell JR et al. In-situ deformation of an open-cell flexible polyurethane foam characterised by 3D computed microtomography. *Journal of Materials Science* 2002; 37(8): 1547–1555. DOI:10.1023/A:1014920902712.

[88] Kumar V, Weller JE, Ma M et al. The Effect of Additives on Microcellular PVC Foams: Part II. Tensile Behaviour. *Cellular Polymers* 1998; 17(5): 350–361.

[89] Rodríguez-Pérez MA, González-Peña JI, Witten N et al. The effect of cell size on the physical properties of crosslinked closed cell polyethylene foams produced by a high pressure nitrogen solution process. *Cellular Polymers* 2002; 21(3): 165–194. DOI:10.1177/026248930202100302.

[90] Sun H, Sur GS and Mark JE. Microcellular foams from polyethersulfone and polyphenylsulfone: Preparation and mechanical properties. *European Polymer Journal* 2002; 38(12): 2373–2381. DOI:10.1016/S0014-3057(02)00149-0.

[91] Fu J, Jo C and Naguib H. The effect of the processing parameters on the mechanical properties of PMMA microcellular foams. *Annual Technical Conference - ANTEC, Conference Proceedings* 2005; 24(4): 134–139.

[92] Bureau MN and Kumar V. Fracture toughness of high density polycarbonate microcellular foams. *Journal of Cellular Plastics* 2006; 42(3): 229–240. DOI:10.1177/0021955X06063512.

[93] Nadella K and Kumar V. Tensile and Flexural Properties of Solid-State Microcellular ABS Panels. In Gdoutos EE (ed.) *Experimental Analysis of Nano and Engineering Materials and Structures*. Dordrecht: Springer Netherlands. ISBN 978-1-4020-6239-1, pp. 765–766. DOI:10.1007/978-1-4020-6239-1_380.

[94] Rodriguez-Perez MA, Lobos J, Perez-Muñoz CA et al. Mechanical behaviour at low strains of LDPE foams with cell sizes in the microcellular range: Advantages of using these materials in structural elements. *Cellular Polymers* 2008; 27(6): 347–362. DOI:10.1177/026248930802700602.

[95] Weller JE and Kumar V. Solid-state microcellular polycarbonate foams. II. the effect of cell size on tensile properties. *Polymer Engineering and Science* 2010; 50(11): 2170–2175. DOI:10.1002/pen.21737.

[96] Miller D and Kumar V. Microcellular and nanocellular solid-state polyetherimide (PEI) foams using sub-critical carbon dioxide II. Tensile and impact properties. *Polymer* 2011; 52(13): 2910–2919. DOI:10.1016/j.polymer.2011.04.049.

[97] Notario B, Pinto J and Rodríguez-Pérez MA. Towards a new generation of polymeric foams: PMMA nanocellular foams with enhanced physical properties. *Polymer* 2015; 63: 116–126. DOI:10.1016/j.polymer.2015.03.003.

[98] Wang G, Zhao J, Wang G et al. Low-density and structure-tunable microcellular PMMA foams with improved thermal-insulation and compressive mechanical properties. *European Polymer Journal* 2017; 95(August): 382–393. DOI:10.1016/j.eurpolymj.2017.08.025.

[99] Wang G, Wan G, Chai J et al. Structure-tunable thermoplastic polyurethane foams fabricated by supercritical carbon dioxide foaming and their compressive mechanical properties. *Journal of Supercritical Fluids* 2019; 149: 127–137. DOI:10.1016/j.supflu.2019.04.004.

[100] Zhang R, Chen J, Zhu Y et al. Correlation between the structure and compressive property of pmma microcellular foams fabricated by supercritical co_2 foaming method. *Polymers* 2020; 12(2). DOI:10.3390/polym12020315.

[101] Pinto J. *Fabrication and Characterization of Nanocellular Polymeric Materials from Nanostructured Polymers*. PhD Thesis, Université de Bordeaux, 2014.

[102] Gibson LJ and Ashby MF. The Mechanics of Three-Dimensional Cellular Materials. *Proceedings of the Royal*

Society A: Mathematical, Physical and Engineering Sciences 1982; 382(1782): 43–59. DOI:10.1098/rspa.1982.0088.

[103] Chan R and Nakamura M. Mechanical Properties of Plastic Foams: The Dependence of Yield Stress and Modulus on the Structural Variables of Closed-Cell and Open-Cell Foams. *Journal of Cellular Plastics* 1969; 5(2): 112–118. DOI: 10.1177/0021955X6900500207.

[104] Baxter S and Jones TT. Physical properties of foamed plastics and their dependence on structure. *Plastics and Polymers* 1972; 40(146): 69.

[105] Brigthon CA and Measey AE. *Expanded PVC*. QMC Industrial Research, 1973.

[106] Viana GM and Carlsson LA. Mechanical Properties and Fracture Characterization of Cross-Linked PVC Foams. *Journal of Sandwich Structures and Materials* 2002; 4(April 2002): 99–113. DOI:10.1106/109963602022227.

[107] Kabir ME, Saha MC and Jeelani S. Tensile and fracture behavior of polymer foams. *Materials Science and Engineering A* 2006; 429(1-2): 225–235. DOI:10.1016/j.msea.2006.05.133.

[108] Waldman FA. *The Processing of Microcellular Foam*. PhD Thesis, Massachusetts Institute of Technology, 1982.

[109] Maiti SK, Ashby MF and Gibson LJ. Fracture toughness of brittle cellular solids. *Scripta Metallurgica* 1984; 18(3): 213–217. DOI:10.1016/0036-9748(84)90510-6.

[110] Traeger RK. Physical Properties of Rigid Polyurethane Foams. *Journal of Cellular Plastics* 1967; 3(9): 405–418. DOI:10.1177/0021955X6700300906.

[111] Matonis VA. Elastic behavior of low density rigid foams in structural applications. *Soc Plast Eng J* 1964; 20: 1024 – 1030.

[112] Patel M and Finnie I. Structural features and mechanical properties of rigid cellular plastics. *J Materials* 1970; 5(909).

[113] Zhang B, Hu S and Fan Z. Anisotropic compressive behavior of functionally density graded aluminum foam prepared by controlled melt foaming process. *Materials* 2018; 11(12). DOI:10.3390/ma11122470.

[114] Glacet A, Réthoré J, Tanguy A et al. On the failure resistance of quasi-periodic lattices. *Scripta Materialia* 2018; 156: 23–26. DOI:10.1016/j.scriptamat.2018.07.001.

[115] Eid E, Seghir R and Réthoré J. Multiscale analysis of brittle failure in heterogeneous materials. *Journal of the Mechanics and Physics of Solids* 2021; 146(September 2020): 0–59. DOI:10.1016/j.jmps.2020.104204.

[116] Kopp JB and Girardot J. Dynamic fracture of a semi-crystalline bio-based polymer pipe: Effect of temperature. *Journal of Minerals and Materials Characterization and Engineering* 2021; 9: 227–244.

[117] Kopp JB, Schmittbuhl J, Noel O et al. Fluctuations of the dynamic fracture energy values related to the amount of created fracture surface. *Engineering Fracture Mechanics* 2014; 126: 178–189. DOI:10.1016/j.engfracmech.2014.05.014.

[118] Fond C and Schirrer R. Influence of crack speed on fracture energy in amorphous and rubber toughened amorphous polymers. *Plastics, Rubber and Composite, Macromolecular Engineering* 1997; 30: 116–124.

[119] Kopp JB and Girardot J. Dynamic fracture in a semicrystalline biobased polymer: An analysis of the fracture surface. *International Journal of Fracture* 2020; 226(1): 121–132. DOI:10.1007/s10704-020-00482-y.

[120] Irwin G, Dally J, Kobayashi T et al. On the determination of $\dot{a} - k$ relationship for birefringent polymers. *Experimental mechanics* 1979; 19: 121–128.

[121] Liu Y, St-Pierre L, Fleck NA et al. High fracture toughness micro-architectured materials. *Journal of the Mechanics and Physics of Solids* 2020; 143: 104060. DOI:10.1016/j.jmps.2020.104060.

[122] Fowlkes CW. Fracture toughness tests of a rigid polyurethane foam. *International Journal of Fracture* 1974; 10(1): 99–108. DOI:10.1007/BF00955084.

[123] McIntyre A and Anderton GE. Fracture properties of a rigid polyurethane foam over a range of densities. *Polymer* 1979; 20(2): 247–253. DOI:10.1016/0032-3861(79)90229-5.

[124] Burman M. *Fatigue Crack Initiation and Propagation in Sandwich Structure*. PhD Thesis, Kungliga Tekniska Högskolan (KTH), 1998. DOI:10.3969/j.issn.1007-7294.2019.08.011.

[125] Saenz EE, Carlsson LA and Karlsson AM. In situ analysis of crack propagation in polymer foams. *Journal of Materials Science* 2011; 46(16): 5487–5494. DOI:10.1007/s10853-011-5491-y.

[126] Legan MA, Kolodezev VE and Sheremet AS. Quasi-brittle fracture of foam-polystyrene plates with hole. *11th International Conference on Fracture 2005, ICF11* 2005; 8: 5893–5898.

[127] Marșavina L and Linul E. Fracture toughness of rigid polymeric foams: A review. *Fatigue and Fracture of Engineering Materials and Structures* 2020; 43(11): 2483–2514. DOI:10.1111/ffe.13327.

[128] Ridha M and Shim VP. Microstructure and tensile mechanical properties of anisotropic rigid polyurethane foam. *Experimental Mechanics* 2008; 48(6): 763–776. DOI: 10.1007/s11340-008-9146-0.

[129] Huang JS and Gibson LJ. Fracture toughness of brittle foams. *Acta Metallurgica Et Materialia* 1991; 39(7): 1627–1636. DOI:10.1016/0956-7151(91)90250-5.

[130] McCullough KY, Fleck NA and Ashby MF. Uniaxial stress-strain behaviour of aluminum alloy foams. *Acta Materialia* 1999; 47(8): 2323–2330. DOI:10.1016/S1359-6454(99)00128-7.

[131] Andrews EW, Gioux G, Onck PR et al. Size effects in ductile cellular solids. Part II: Experimental results. *International Journal of Mechanical Sciences* 2001; 43(3): 701–713. DOI: 10.1016/S0020-7403(00)00043-6.

[132] Olurin OB, Fleck NA and Ashby MF. Deformation and fracture of aluminium foams. *Materials Science and Engineering A* 2000; 291(1-2): 136–146. DOI:10.1016/S0921-5093(00)00954-0.

[133] Motz C and Pippan R. Deformation behaviour of closed-cell aluminium foams in tension. *Acta Materialia* 2001; 49(13): 2463–2470. DOI:10.1016/S1359-6454(01)00152-5.

[134] Fleck NA, Olurin OB, Chen C et al. The effect of hole size upon the strength of metallic and polymeric foams. *Journal of the Mechanics and Physics of Solids* 2001; 49(9): 2015–2030. DOI:10.1016/S0022-5096(01)00033-3.

[135] Motz C. *Brucheigenschaften Und Bruchzähigkeit von Duktilen, Metallischen Schäumen*. PhD Thesis, Institut für Metallphysik der Montanuniversität Leoben, 2002.

[136] Dillard T, N 'guyen F, Forest S et al. In-situ X-ray microtomography tensile tests in ductile open- cell nickel foams. *Cellular Metals and Metal Foaming Technology* 2003; .

[137] Colombo P and Degischer HP. Highly porous metals and ceramics. *Advanced Engineering Materials* 2012; 14(12): 1051. DOI:10.1002/adem.201200347.

[138] Le Barbenchon L, Kopp JB, Girardot J et al. Reinforcement of cellular materials with short fibres: Application to a bio-based cork multi-scale foam. *Mechanics of Materials* 2020; 142(October 2019): 103271. DOI:10.1016/j.mechmat.2019.103271.

[139] Marsavina L. Fracture mechanics of cellular solids. *CISM International Centre for Mechanical Sciences, Courses and Lectures* 2010; 521: 1–46. DOI:10.1007/978-3-7091-0297-8_1.

[140] Anderton GE. Fracture properties of rigid polyurethane foams. *Journal of Applied Polymer Science* 1975; 19(12): 3355–3359. DOI:10.1002/app.1975.070191219.

[141] Anderson TL. *Fracture Mechanics: Fundamentals and Applications (3rd ed.)*. Boca Raton: CRC Press, 2005.

[142] Nilsson F. Dynamic stress-intensity factors for finite strip problems. *International Journal of Fracture* 1972; 8: 403–411.

[143] LANGE FF and MILLER KT. Open-Cell, Low-Density Ceramics Fabricated from Reticulated Polymer Substrates. *Advanced Ceramic Materials* 1987; 2(4): 827–831. DOI:10.1111/j.1551-2916.1987.tb00156.x.

[144] Brezny R, Green DJ and Dam CQ. Evaluation of Strut Strength in Open-Cell Ceramics. *Journal of the American Ceramic Society* 1989; 72(6): 885–889. DOI:10.1111/j.1151-2916.1989.tb06239.x.

[145] Brezny R and Green DJ. Fracture Behavior of Open Cell Ceramics. *MRS Proceedings* 1990; 207. DOI:10.1557/proc-207-3.

[146] Brezny R and Green DJ. The effect of cell size on the mechanical behavior of cellular materials. *Acta Metallurgica Et Materialia* 1990; 38(12): 2517–2526. DOI:10.1016/0956-7151(90)90263-G.

[147] Brezny R and Green DJ. Fracture Behaviour of Open Cell Ceramics. *Mat Res Soc Symp Proc* 1991; 207.

[148] ASTM. Standard Test Method for Tensile Properties of Plastics, 2022. DOI:10.1520/D0638-14.

[149] Kumar V and Weller JE. The Effect of Cell Size on the Tensile Behavior of Microcellular Polycarbonate. In *ASME 1996 International Mechanical Engineering Congress and Exposition*. American Society of Mechanical Engineers Digital Collection, pp. 17–25. DOI:10.1115/IMECE1996-1404.

[150] Linul E, Marşavina L, Sadowski T et al. Size effect on fracture toughness of rigid polyurethane foams. *Solid State Phenomena* 2012; 188: 205–210. DOI:10.4028/www.scientific.net/SSP.188.205.

[151] Kidane A. On the Failure and Fracture of Polymer Foam Containing Discontinuities. *ISRN Materials Science* 2013; 2013: 1–9. DOI:10.1155/2013/408596.

[152] Touliatou D and Wheel MA. K-dominance and size effect in mode I fracture of brittle materials with low to medium porosity. *Engineering Fracture Mechanics* 2018; 201(June): 269–281. DOI:10.1016/j.engfracmech.2018.06.041.

[153] Poapongsakorn P and Carlsson LA. Fracture toughness of closed-cell PVC foam: Effects of loading configuration and cell size. *Composite Structures* 2013; 102: 1–8. DOI:10.1016/j.compstruct.2013.02.023.

[154] Marsavina L, Constantinescu DM, Linul E et al. Refinements on fracture toughness of PUR foams. *Engineering Fracture Mechanics* 2014; 129: 54–66. DOI:10.1016/j.engfracmech.2013.12.006.

[155] Marsavina L and Constantinescu DM. *Failure and Damage in Cellular Materials*, volume 560. CISM International Centre for Mechanical Sciences, 2015. ISBN 978-3-7091-1835-1. DOI:10.1007/978-3-7091-1835-1_3.

[156] Jin H, Lu Wy, Hong S et al. Fracture behavior of polyurethane foams. In *2007 ASME International Mechanical Engineering Congress and Exposition*. Seattle, pp. 4–7.

[157] Marsavina L, Linul E, Voiconi T et al. A comparison between dynamic and static fracture toughness of polyurethane foams. *Polymer Testing* 2013; 32(4): 673–680. DOI:10.1016/j.polymertesting.2013.03.013.

[158] Jelitto H and Schneider GA. Fracture toughness of porous materials – Experimental methods and data. *Data in Brief* 2019; 23: 103709. DOI:10.1016/j.dib.2019.103709.

[159] Jelitto H and Schneider GA. A geometric model for the fracture toughness of porous materials. *Acta Materialia* 2018; 151: 443–453. DOI:10.1016/j.actamat.2018.03.018.

[160] Jelitto H and Schneider GA. Extended cubic fracture model for porous materials and the dependence of the fracture toughness on the pore size. *Materialia* 2020; 12(May): 100761. DOI:10.1016/j.mtla.2020.100761.

[161] Green DJ. Fabrication and Mechanical Properties of Lightweight Ceramics Produced by Sintering of Hollow Spheres. *Journal of the American Ceramic Society* 1985; 68(7): 403–409. DOI:10.1111/j.1151-2916.1985.tb10153.x.

[162] Choi S and Sankar BV. A micromechanical method to predict the fracture toughness of cellular materials. *International Journal of Solids and Structures* 2005; 42(5-6): 1797–1817. DOI:10.1016/j.ijsolstr.2004.08.021.

[163] Mills NJ and Kang P. The Effect of Water Immersion on the Mechanical Properties of Polystyrene Bead Foam Used in Soft Shell Cycle Helmets. *Journal of Cellular Plastics* 1994; 30(3): 196–222. DOI:10.1177/0021955X9403000301.

[164] Marsavina L and Sadowski T. Dynamic fracture toughness of polyurethane foam. *Polymer Testing* 2008; 27(8): 941–944. DOI:10.1016/j.polymertesting.2008.08.006.

[165] Mills NJ. Modeling the dynamic crushing of closed-cell polyethylene and polystyrene foams. *Journal of Cellular Plastics* 2011; 47(2): 173–197. DOI:10.1177/0021955X10397765.

[166] de Souza FM, Desai Y and Gupta RK. Introduction to Polymeric Foams. In *Polymeric Foams: Fundamentals and Types of Foams (Volume 1)*, *ACS Symposium Series*, volume 1439, chapter 1. American Chemical Society, 2023. pp. 1–23. DOI:10.1021/bk-2023-1439.ch001.

[167] Collias DI and Baird DG. Impact behavior of microcellular foams of polystyrene and styrene-acrylonitrile copolymer, and single-edge-notched tensile toughness of microcellular foams of polystyrene, styrene-acrylonitrile copolymer, and palycarbonate. *Polymer Engineering & Science* 1995; 35(14): 1178–1183. DOI:10.1002/pen.760351408.

[168] Determination of Charpy impact properties - Part 1: Non-instrumented impact test. Standard, International Organization for Standardization, Geneva, CH, 2010.

[169] Standard Test Methods for Impact Resistance of Plastic Film by the Free-Falling Dart Method. Standard, ASTM International, USA, 2022.

[170] Standard Test Methods for Determining the Izod Pendulum Impact Resistance of Plastics. Standard, ASTM International, USA, 1993.

[171] Collias DI, Baird DG and Borggreve RJ. Impact toughening of polycarbonate by microcellular foaming. *Polymer* 1994; 35(18): 3978–3983. DOI:10.1016/0032-3861(94)90283-6.

[172] Saiz-Arroyo C, Rodríguez-Pérez MA, Tirado J et al. Structure-property relationships of medium-density polypropylene foams. *Polymer International* 2013; 62(9): 1324–1333. DOI:10.1002/pi.4424.

[173] Juntunen R, Kumar V, Weller J et al. Impact strength of high density microcellular poly(vinyl chloride) foams. *Journal of Vinyl and Additive Technology* 2000; 6(2). DOI: 10.1002/vnl.10230.

[174] Avalle M and Scattina A. Mechanical properties and impact behavior of a microcellular structural foam. *Latin American Journal of Solids and Structures* 2014; 11(2): 200–222. DOI: 10.1590/S1679-78252014000200004.

[175] Kumar V, Juntunen RP and Barlow C. Impact strength of high relative density solid state carbon dioxide blown crystallizable poly(ethylene terephthalate) microcellular foams. *Cellular Polymers* 2000; .

[176] Cuadra-Rodríguez D, Barroso-Solares S, Laguna-Gutiérrez E et al. Opening Pores and Extending the Application Window: Open-Cell Nanocellular Foams. *Macromolecular Materials and Engineering* 2023; n/a(n/a): 2300087. DOI: 10.1002/mame.202300087.

[177] Martín de Leon J. *Master Thesis : Study of the Process - Density - Structure Relationship in Low Density Nanocellular Materials Based on PMMA . Presented By :*. PhD Thesis, Universidad de Valladolid, 2016.

[178] Pinto J, Notario B, Verdejo R et al. Molecular confinement of solid and gaseous phases of self-standing bulk nanoporous polymers inducing enhanced and unexpected physical properties. *Polymer* 2017; 113: 27–33. DOI:10.1016/j.polymer.2017.02.046.

[179] Pinto J, Notario B, Verdejo R et al. Molecular confinement of solid and gaseous phases of self-standing bulk nanoporous polymers inducing enhanced and unexpected physical properties. *Polymer* 2017; 113: 27–33. DOI:10.1016/j.polymer.2017.02.046.

[180] Kraus J, Müller-Buschbaum P, Kuhlmann T et al. Confinement effects on the chain conformation in thin polymer films. *Europhysics Letters* 2000; 49(2): 210–216. DOI:10.1209/epl/i2000-00135-4.

[181] Kirste RG, Kruse WA and Ibel K. Determination of the conformation of polymers in the amorphous solid state and in concentrated solution by neutron diffraction. *Polymer* 1975; 16(2): 120–124. DOI:10.1016/0032-3861(75)90140-8.

[182] Keddie JL, Jones RAL and Cory RA. Interface and surface effects on the glass-transition temperature in thin polymer films. *Faraday Discussions* 1994; 98(0): 219–230. DOI: 10.1039/FD9949800219.

[183] Hartmann L, Gorbatschow W, Hauwede J et al. Molecular dynamics in thin films of isotactic poly(methyl methacrylate). *The European Physical Journal E* 2002; 8(2): 145–154. DOI:10.1140/epje/i2001-10073-y.

[184] Kremer F, Tress M and Mapesa EU. Glassy dynamics and glass transition in nanometric layers and films: A silver lining on the horizon. *Journal of Non-Crystalline Solids* 2015; 407: 277–283. DOI:10.1016/j.jnoncrysol.2014.08.016.

[185] Forrest J and Dalnoki-Veress K. The glass transition in thin polymer films. *Advances in Colloid and Interface Science* 2001; 94: 167–195.

[186] Roth CB and Dutcher JR. Glass transition and chain mobility in thin polymer films. *Journal of Electroanalytical Chemistry* 2005; 584: 13–22.

[187] Stafford C, Vogt B, Harrison C et al. Elastic moduli of ultrathin amorphous polymer films. *Macromolecules* 2006; 39: 5095–5099.

[188] Mapesa EU, Shahidi N, Kremer F et al. Interfacial Dynamics in Supported Ultrathin Polymer Films—From the Solid to the Free Interface. *The Journal of Physical Chemistry Letters* 2021; 12(1): 117–125. DOI:10.1021/acs.jpclett.0c03211.

[189] Borggreve RJ, Gaymans RJ and Eichenwald HM. Impact behaviour of nylon-rubber blends: 6. Influence of structure on voiding processes; toughening mechanism. *Polymer* 1989; 30(1).

[190] Shaikeea AJD, Cui H, O'Masta M et al. The toughness of mechanical metamaterials. *Nature Materials* 2022; 21(3): 297–304. DOI:10.1038/s41563-021-01182-1.

[191] Quintana-Alonso I and Fleck NA. Fracture of brittle lattice materials: A review. *Major Accomplishments in Composite Materials and Sandwich Structures: An Anthology of ONR Sponsored Research* 2009; : 799–816DOI:10.1007/978-90-481-3141-9_30.

[192] Tankasala HC, Deshpande VS and Fleck NA. 2013 koiter medal paper: Crack-tip fields and toughness of two-dimensional elastoplastic lattices. *Journal of Applied Mechanics, Transactions ASME* 2015; 82(9). DOI:10.1115/1.4030666.

[193] O'Masta MR, Dong L, St-Pierre L et al. The fracture toughness of octet-truss lattices. *Journal of the Mechanics and Physics of Solids* 2017; 98(April 2016): 271–289. DOI: 10.1016/j.jmps.2016.09.009.

[194] Wu Y and Yang L. Size and topology effects on fracture behavior of cellular structures. *Solid Freeform Fabrication 2018: Proceedings of the 29th Annual International Solid Freeform Fabrication Symposium - An Additive Manufacturing Conference, SFF 2018* 2020; : 821–834.